The mitochondrial ribosomal protein L13 is critical for the structural and functional integrity of the mitochondrion in *Plasmodium falciparum*

Hangjun Ke[1], Swati Dass, Joanne M. Morrisey, Michael W. Mather, and Akhil B. Vaidya

From the Center for Molecular Parasitology, Department of Microbiology and Immunology, Drexel University College of Medicine, Philadelphia, Pennsylvania 19129

Edited by John M. Denu

The phylum Apicomplexa contains a group of protozoa causing diseases in humans and livestock. *Plasmodium* spp., the causative agent of malaria, contains a mitochondrion that is very divergent from that of their hosts. The malarial mitochondrion is a clinically validated target for the antimalarial drug atovaquone, which specifically blocks the electron transfer activity of the bc_1 complex of the mitochondrial electron transport chain (mtETC). Most mtETC proteins are nuclear-encoded and imported from the cytosol, but three key protein subunits are encoded in the *Plasmodium* mitochondrial genome: cyt *b*, COXI, and COXIII. They are translated inside the mitochondrion by mitochondrial ribosomes (mitoribosomes). Here, we characterize the function of one large mitoribosomal protein in *Plasmodium falciparum*, PfmRPL13. We found that PfmRPL13 localizes to the parasite mitochondrion and is refractory to genetic knockout. Ablation of PfmRPL13 using a conditional knockdown system (TetR-DOZI-aptamer) caused a series of adverse events in the parasite, including mtETC deficiency, loss of mitochondrial membrane potential ($\Delta\psi_m$), and death. The PfmRPL13 knockdown parasite also became hypersensitive to proguanil, a drug proposed to target an alternative process for maintaining $\Delta\psi_m$. Surprisingly, transmission EM revealed that PfmRPL13 disruption also resulted in an unusually elongated and branched mitochondrion. The growth arrest of the knockdown parasite could be rescued with a second copy of PfmRPL13, but not by supplementation with decylubiquinone or addition of a yeast dihydroorotate dehydrogenase gene. In summary, we provide first and direct evidence that mitoribosomes are essential for malaria parasites to maintain the structural and functional integrity of the mitochondrion.

Malaria remains a severe infectious disease in the tropical and subtropical regions of the world, causing millions of clinical cases and taking the lives of half a million people in 2016 (1).

The causative agents, parasites of *Plasmodium* spp., have three genomes localized in three distinct cellular compartments, the nucleus, the apicoplast, and the mitochondrion. The nuclear genome is composed of 14 chromosomes (23 mega base pairs) and encodes ~5500 proteins (2). The apicoplast is a relict plastid derived from primary and secondary endosymbiosis, which contains a circular bacterial like DNA (35 kb), encoding ~30 proteins, 2 rRNA genes (16S and 23S), and a complete set of tRNAs required for protein translation within this organelle (3, 4).

The mitochondria of all eukaryotic organisms are believed to be derived from one single common ancestor, an α-protobacterium (5). In apicomplexan parasites, the mitochondrial genomes tend to be small, 6–11 kb in length (6, 7). In one genus, *Cryptosporidium*, the mitochondrial genome has been entirely lost (8). The mitochondrial DNA (mtDNA)[2] of malaria parasites is only 6 kb, encoding three proteins of the mitochondrial electron transport chain (mtETC): cytochrome (cyt) *b*, cyt *c* oxidase subunits I and III (COX I and III) (6, 9, 10). These three proteins are translated by the mitochondrial ribosomes (mitoribosomes). The 6 kb mtDNA also encodes mitochondrial rRNA genes; however, these rRNAs are highly fragmented (~30 small pieces of 20–200 bp) and scattered throughout the mitochondrial genome (11–13). It remains entirely unknown how these many small rRNA pieces come together to form a working mitoribosomal complex. Another striking feature of the malarial mtDNA is that it does not encode any tRNA genes, and mitochondrial tRNAs have to be imported from the cytosol (14).

To translate genes encoded on three distinctive genomes localized in three cellular compartments, *Plasmodium* parasites utilize three types of ribosomes. The cytosolic 80S ribosomes are numerous in the parasite cytoplasm and were easily detected by transmission EM studies carried out more than 50 years ago (15). Their structure has just been resolved by cryo–electron microscopy (cryo-EM) (16, 17). The ribosomes in the apicoplast and mitochondrion of malaria parasites are both prokaryotic type; yet, they possess unique features that are distinct from bacterial ribosomes or organellar ribosomes of other

[1] To whom correspondence should be addressed: 2900 Queen Lane, Philadelphia, PA 19129. Tel.: 215-991-8448; Fax: 215-848-2271; E-mail: hk84@drexel.edu.

[2] The abbreviations used are: mtDNA, mitochondrial DNA; mtETC, mitochondrial electron transport chain; cyt, cytochrome; LSU, large subunit; cryo-EM, cryo–electron microscopy; DHODH, dihydroorotate dehydrogenase; aTc, anhydrotetracycline; gRNA, guider RNA; IDC, intraerythrocytic developmental cycle; TEM, transmission EM; Qd, decylubiquinone; TetR, tetracycline repressor; 3HA, triple HA.

SASBMB

eukaryotes (18). It has been shown that active protein translation occurs in the apicoplast, which renders malaria parasites sensitive to several antibiotics (19–22). In contrast, the mitochondrial protein translation system in *Plasmodium* has remained an enigma for a long time. On one hand, direct evidence for mitochondrial protein translation in the parasites or in the entire Apicomplexa phylum is lacking, but on the other hand, the essentiality of the mtETC (23, 24) and the appearance of cyt *b* mutations conferring atovaquone resistance (25) strongly imply that the mitochondrial ribosomes are active.

In this study, we have characterized one conserved large subunit (LSU) protein of mitoribosomes in *Plasmodium falciparum* (PfmRPL13, PF3D7_0214200). It has been shown that L13 is a critical component involved in the first step of ribosome LSU assembly in bacteria (26) and is one of the eight LSU subunits required to form a minimal subribosomal particle maintaining peptidyltransferase activity in *Thermus aquaticus* (27). Here, for the first time, we provide direct evidence that PfmRPL13 is essential for malaria parasites, highlighting the significance of mitoribosomes for parasite physiology and survival.

Results

PfmRPL13 is essential in asexual blood stages of P. falciparum

PF3D7_0214200 (designated as PfmRPL13) is annotated as the putative mitochondrial ribosomal protein L13 in *P. falciparum* (www.plasmodb.org)[3] (47). To compare the sequence similarity (or divergence) of mitochondrial ribosomal L13 proteins from various organisms, we performed a multiple sequence alignment and maximum likelihood phylogenetic analysis. As shown in Fig. S1, PfmRPL13 is closely related to its orthologues in other apicomplexan parasites, but shares much less sequence similarity to other mitoribosomal L13 proteins. PfmRPL13 and *Toxoplasma* mRPL13 share 55% identical residues, but the percent identity between the *P. falciparum* and human proteins is 23%, as calculated from the alignment (Fig. S1*A*). As might be expected then, in the phylogenetic results the apicomplexan mRPL13s form a separate, well-supported clade within the overall mitochondrial L13 grouping (Fig. S1*B*).

To verify the subcellular localization of PfmRPL13 in *P. falciparum*, we integrated a copy of PfmRPL13 tagged with triple HA (3HA) or GFP into the genome of Dd2attB parasites (28). Interestingly, Dd2attB transfected with the pLN-PfmRPL13-GFP construct grew very slowly and did not express GFP, as determined by fluorescence microscopy and Western blotting (data not shown), suggesting that expression of the PfmRPL13-GFP fusion protein was silenced by some unknown mechanism(s). However, Dd2attB transfected with the pLN-PfmRPL13-3HA construct expressed PfmRPL13-3HA. Immunofluorescence assay showed that PfmRPL13-3HA was localized in the parasite mitochondria with almost no signal in other cellular compartments (Fig. 1). Importantly, Dd2attB-PfmRPL13-3HA grew normally as compared with the parental line (data not shown). Based on its evolutionary sequence con-
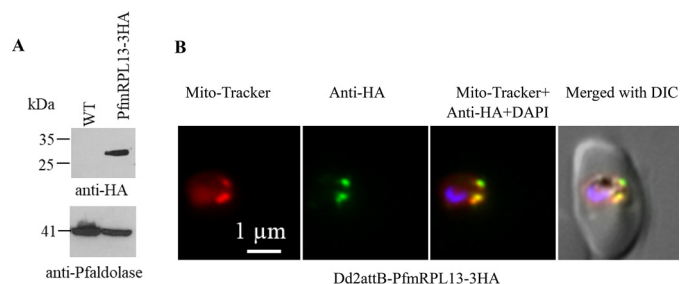

Figure 1. Expression and localization of PfmRPL13 in *P. falciparum*. *A*, expression of PfmRPL13–3HA in Dd2attB parasites was confirmed by Western blotting. *P. falciparum* aldolase (41 kDa) served as a loading control. *B*, PfmRPL13–3HA was localized in the parasite mitochondria as revealed by immunofluorescence assays.

servation (29) and mitochondrial localization, we conclude that PF3D7_0214200 is very likely to be the mitoribosomal large subunit protein L13 in *P. falciparum*.

To verify whether PfmRPL13 is essential for parasite growth in asexual blood stages, we attempted to knock it out in two WT lines, D10 and NF54, via a CRISPR/Cas9-mediated approach (see "Materials and methods" in the supporting information). Transfections in these lines were performed with circular or linearized template plasmids along with pUF1-Cas9 and selected with either a single drug for the template plasmid or two drugs for both the template and Cas9 plasmids ("Materials and methods"). In cultures transfected with a circular template plasmid, negative selection against maintenance of the plasmid was also performed ("Materials and methods"). However, despite multiple attempts, gene knockout was unsuccessful (data not shown). Because it has been shown that the only essential role of the mtETC in asexual blood stages is to provide an electron sink for the parasite dihydroorotate dehydrogenase (DHODH), which is essential for pyrimidine biosynthesis (23), we hypothesized that PfmRPL13 might be dispensable in the yeast DHODH (yDHODH) transgenic parasites, which do not require a functional mtETC. Knockout approaches as described above were carried out in the NF54attB-yDHODH-GFP line which carries a fusion protein of yDHODH and GFP. Gene knockout in this line was not successful after many attempts, however. In summary, PfmRPL13 is refractory to gene disruption, suggesting that PfmRPL13 is likely to be essential.

Because our knockout studies were unable to definitely determine the essentiality of PfmRPL13 in the parasites, we utilized a recently developed translational knockdown approach, the TetR-DOZI-aptamer system (30). In this system, protein translation is conditionally regulated by addition of anhydrotetracycline (aTc) (ON) or withdrawal of aTc (OFF). As shown in Fig. 2*A*, the TetR-DOZI-aptamer system was inserted into the genomic locus by double crossover recombination facilitated by CRISPR/Cas9 ("Materials and methods"). We transfected D10 WT parasites with a linearized template vector and two circular guider RNA (gRNA) constructs ("Materials and methods"), selected with blasticidin and aTc, and obtained transgenic parasites 3 weeks post electroporation. As shown in Fig. 2*B*, the genomic locus of PfmRPL13 was confirmed to be correctly modified in the transgenic parasites by diagnostic PCR analysis. We named this line D10-PfmRPL13-KD (knock-

---

[3] Please note that the JBC is not responsible for the long-term archiving and maintenance of this site or any other third party hosted site.
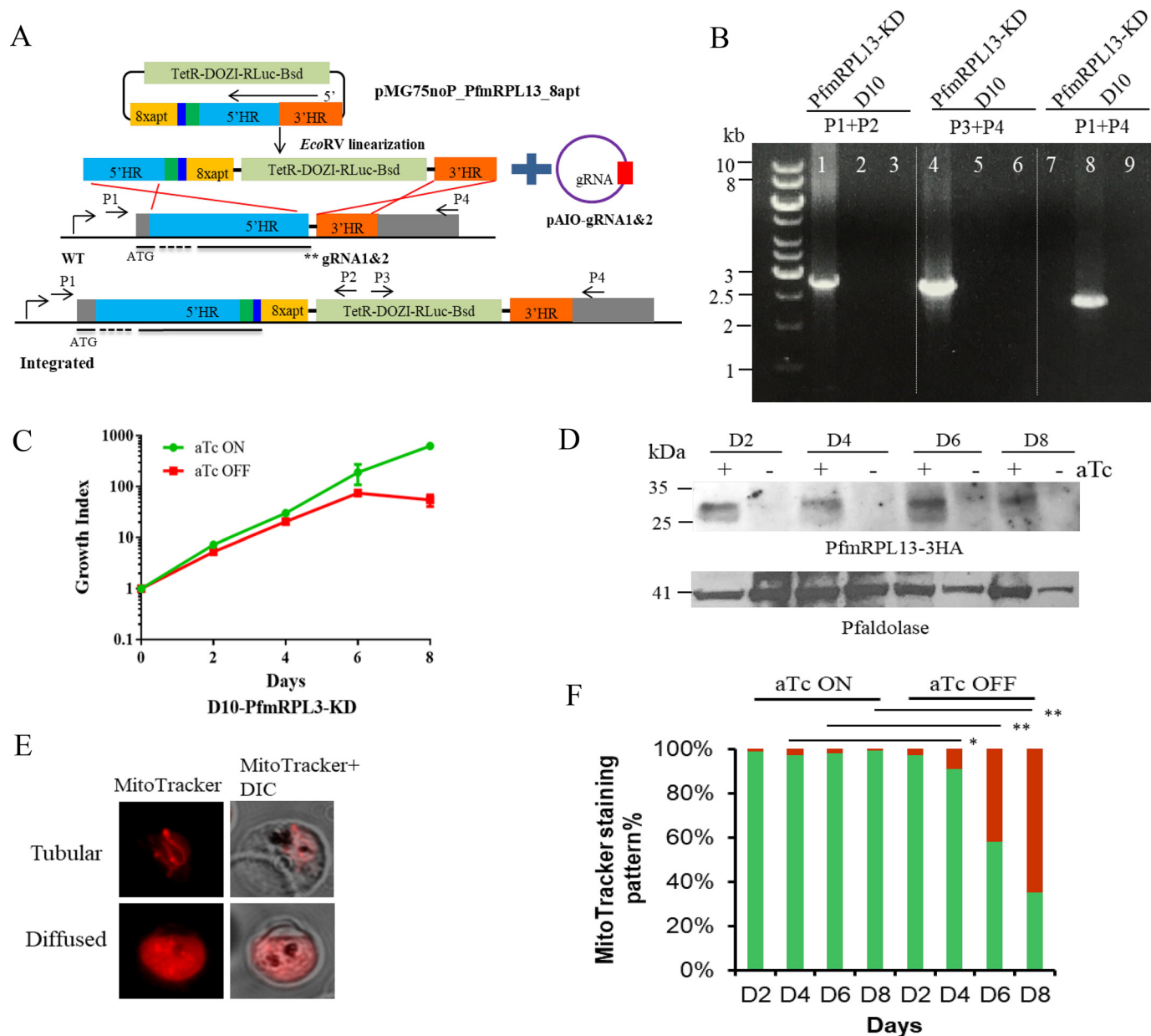
Figure 2. Genetic ablation of PfmRPL13 through the TetR-DOZI-aptamer system facilitated with CRISPR/Cas9. *A*, the TetR-DOZI-aptamer system (30) was inserted into the PfmRPL13 genetic locus through a double crossover recombination strategy facilitated by a CRISPR/Cas9 system. TetR-DOZI-RLuc-Bsd is the combined gene for a fusion protein of tetracycline repressor with development of zygote inhibited (DOZI), followed by Renilla luciferase and blasticidin deaminase. *8xapt* stands for 8 copies of TetR-binding aptamers. *5'HR* and *3'HR* are upstream and downstream homologous regions of the PfmRPL13 gene. The *green box* next to 5'HR indicates shield mutations that keep amino acid sequences intact but change nucleotide sequences to avoid repetitive cutting by Cas9. The *dark blue box* next to the *green box* is the 3HA tag. The template plasmid was fully digested with EcoRV before electroporation. Two gRNAs (**) adjacent to the stop codon of PfmRPL13 were cloned into the pAIO plasmid individually. The *black bars* underneath WT and integrated gene models indicate exons of the gene whereas *dashed lines* indicate the introns. *B*, the genotype of the PfmRPL13 knockdown line was verified by diagnostic PCR analysis. D10 genomic DNA served as a control. The sequences of primers P1–P4 are shown in Table S1 and their approximate positions are marked in (*A*). Lanes *1*, *4*, and *7* are products from PCR reactions with template DNA from the D10-PfmRPL13-KD line; lanes *2*, *5*, and *8* with DNA from D10 WT; lanes *3*, *6*, and *9* are no DNA controls. In lane *7*, the fragment to be amplified was too big to work in PCR (>11 kb). *C*, a representative growth curve of the PfmRPL13 knockdown line grown in the presence or absence of aTc (250 nM). Cultures were split 1:5 on days 2, 4, 6, and 8. Parasitemia was determined under a light microscope by counting more than 1000 red blood cells in each Giemsa-stained thin blood smear. Growth index is the cumulative -fold expansion which is the multiplication of parasitemia and split factors over the time course. A split factor is 5 in a 1:5 split. Data shown are the mean ± S.D. of biological replicates. This experiment has been repeated more than 10 times. aTc, anhydrotetracycline. *D*, expression of PfmRPL13–3HA in the knockdown parasites maintained with and without aTc for 8 days was examined by Western blotting. The molecular mass of PfmRPL13–3HA is 28 kDa. *P. falciparum* aldolase (41 kDa) served as a loading control. *E*, MitoTracker staining patterns of healthy *versus* parasites with depolarized mitochondria. *F*, quantification of mitochondrial staining patterns in the PfmRPL13 knockdown line maintained with or without aTc, respectively. *Green bars*, tubular. *Red bars*, diffused. Data shown are averaged from $n = 3$ experiments and analyzed by a Student's *t* test. **, $p < 0.01$; *, $p < 0.05$.

down). It has been shown that protein knockdown efficiency in the TetR-DOZI-aptamer system is determined by aptamer copy number, but aptamers are not very stable (31). To delin-

eate aptamer copy numbers in D10-PfmRPL13-KD, the PCR product of 5′ integration (*lane 1* in Fig. 2*B*) was sequenced and all 8 aptamer copies were intact (data not shown).

The expression of PfmRPL13 was then controlled by addition and removal of aTc in the culture. To rule out any possibility that aTc itself would interfere with parasite growth, the WT D10 line was exposed to media supplemented with aTc (250 nM) and no aTc for 2 weeks but no differences between the two were noticed (data not shown), suggesting that aTc did not alter parasite growth. To determine the effect of knocking down PfmRPL13 on parasite survival, D10-PfmRPL13-KD parasites grown under aTc were enriched by a Percoll gradient, washed thoroughly, and exposed to medium with or without aTc (250 nM) for several intraerythrocytic developmental cycles (IDCs) ("Materials and methods"). As shown in Fig. 2C, D10-PfmRPL13-KD exhibited a severe growth arrest when aTc was removed for three cycles or more. When aTc was removed for more than four cycles, the parasitemia dropped down to a negligible level. To assess parasite growth long term, the aTc-minus culture of D10-PfmRPL13-KD was maintained up to 1 month (split weekly), and growth arrest was maintained for the entire period (data not shown). In the first two cycles post aTc removal, however, the differences between aTc-plus and aTc-minus cultures were not significant under microscopic examination. We then compared their growth rates through [^{3}H]hypoxanthine incorporation assays by titrating aTc in a serial dilution ("Materials and methods"). As shown in Fig. S2, in the first cycle, D10-PfmRPL13-KD incorporated similar levels of [^{3}H]hypoxanthine in low and high concentrations of aTc; however, in the second cycle, the knockdown parasite grown at the lowest aTc concentration (0.24 nM) had a 40% reduction in [^{3}H]hypoxanthine incorporation compared with that of a high aTc (250 nM) culture. In thin blood smears, morphologically deteriorating parasites were observed when aTc was removed for two cycles and the number of morphologically unhealthy parasites increased substantially after removal of aTc for three or more cycles (Fig. S3).

To determine PfmRPL13 expression levels in the knockdown parasites, a knockdown assay was set up using the same protocol as described above. Protein samples were collected every 2 days over four IDCs and examined by Western blotting ("Materials and methods"). As shown in Fig. 2D, PfmRPL13 expression was substantially diminished after aTc was removed for just one cycle. We then qualitatively monitored $\Delta\psi_m$ using MitoTracker in the knockdown parasites maintained with or without aTc ("Materials and methods"). As shown in Fig. 2E, a healthy mitochondrion in a late trophozoite has a tubular structure with MitoTracker staining largely confined to the organelle (*Tubular*, *top panel*), whereas a sick parasite was unable to constrain MitoTracker staining to the mitochondrion, and it diffused throughout the cytosol (*Diffused, bottom panel*). We quantified the percentages of Tubular (healthy) *versus* Diffused (sick) MitoTracker staining patterns in the PfmRPL13 knockdown parasites over four IDCs. As shown in Fig. 2F, D10-PfmRPL13-KD parasites grown with aTc continuously present maintained healthy mitochondria, with very few parasites showing a diffused pattern. However, when aTc was removed, the percentage of parasites with diffused staining in the PfmRPL13 knockdown parasites increased dramatically in the third and fourth cycles. These data suggest that PfmRPL13 and, hence, functional mitoribosomes were critical to maintain

mitochondrial membrane potential and parasite health. Taken together, our data strongly imply that PfmRPL13 is essential for parasite growth and survival in the asexual blood stages of *P. falciparum*. In addition, our results agree with the recent genome-wide gene disruption study carried out in the rodent parasite, which revealed the essentiality of mitochondrial ribosomal protein L13 in *P. berghei* (32).

Genetic ablation of PfmRPL13 leads to mtETC deficiency and proguanil hypersensitivity

Because the mtETC is the recipient of the three proteins translated by mitoribosomes in malaria parasites, it is critical to evaluate the function of the mtETC in the PfmRPL13 knockdown parasites. To do that, we directly measured the bc_1 complex enzymatic activity *in vitro* by an assay measuring its ability to reduce oxidized cyt *c* (a model of Q cycle (33) was depicted in Fig. 3A). We isolated mitochondria from D10-PfmRPL13-KD parasites maintained under aTc continuously and in the absence of aTc for two cycles and four cycles ("Materials and methods"). As shown in Fig. 3B, when aTc was removed for two cycles, there was a ~20% reduction in the bc_1 complex enzymatic activity ($p < 0.05$); however, after aTc was removed for four cycles, the bc_1 complex enzymatic activity was diminished by 70% ($p < 0.001$). These data provide direct evidence that knocking down PfmRPL13 results in defects in the bc_1 complex. It has been shown that whereas yDHODH transgenic parasites are resistant to atovaquone and other bc_1 complex inhibitors, they become hypersensitive to proguanil when their mtETC is chemically inhibited (23). To explore whether mtETC malfunction in the PfmRPL13 knockdown parasites would also make these parasites hypersensitive to proguanil, we cultured the parasites in the absence of aTc for three IDCs and performed a [^{3}H]hypoxanthine incorporation assay. As shown in Fig. 3C, in the WT D10 line, there was no change in proguanil EC$_{50}$s in the presence or absence of aTc (250 nM), suggesting that aTc did not affect proguanil sensitivity. However, in the knockdown parasite, there was a 55-fold increase in proguanil sensitivity when PfmRPL13 was genetically abolished. The EC$_{50}$ of proguanil in D10-PfmRPL13-KD parasites was 9.56 μM with aTc present, whereas it was reduced to 0.17 μM when aTc had been previously removed for three cycles. The yDHODH transgenic line was used as a positive control in the assay (23). As expected, the yDHODH line exhibited proguanil hypersensitivity when the parasite was added with 50 nM atovaquone (Fig. 3C). Remarkably, the level of proguanil hypersensitivity in our PfmRPL13 knockdown parasites (55-fold) was comparable with that of the yDHODH line under atovaquone treatment (62-fold). These data suggest that PfmRPL13 genetic ablation caused a severe mtETC deficiency in a degree that was similar to that triggered by atovaquone inhibition. To rule out the possibility that hypersensitivity to proguanil in the D10-PfmRPL13-KD line was merely a result of poor parasite growth in the absence of aTc, we tested its sensitivity to other antimalarial compounds including PA21A092 (34), a PfATP4 disruptor, and artemisinin. As shown in Fig. S4, in the presence or absence of aTc, D10-PfmRPL13-KD parasites exhibited the same levels of sensitivity to PA21A092 and artemisinin, respectively. Taken together, these data strongly
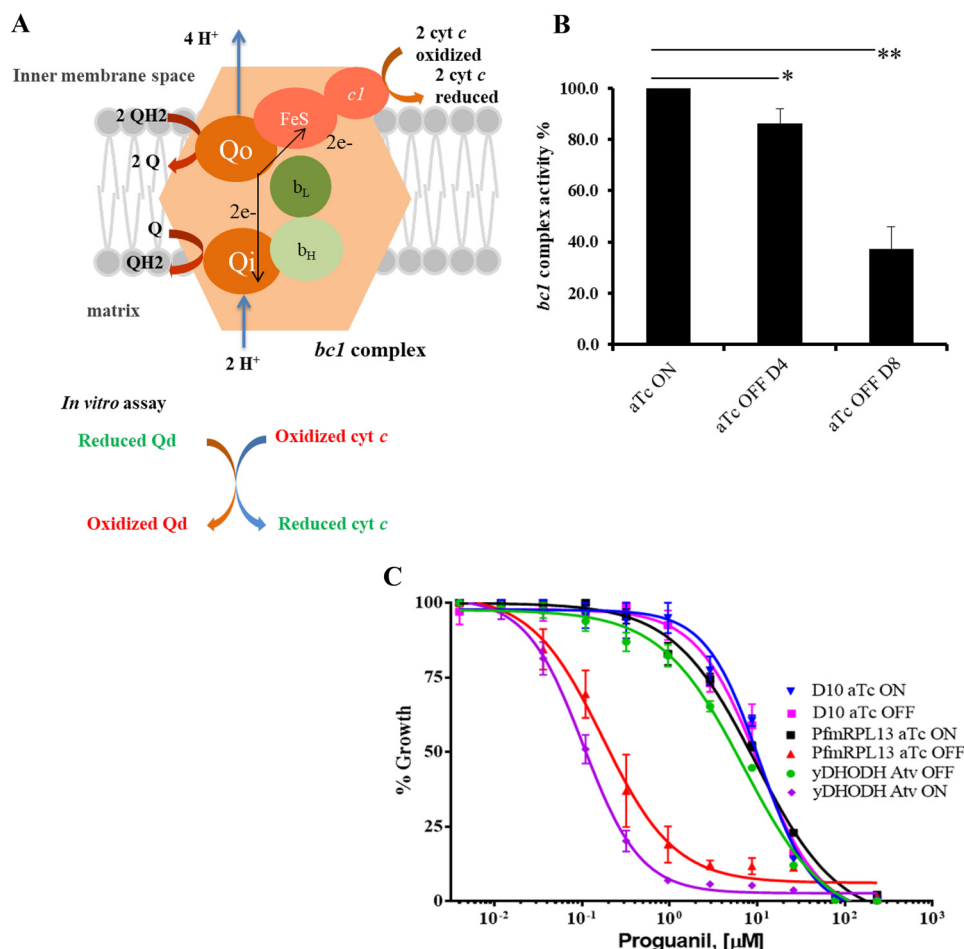
Figure 3. Reduced cytochrome bc_1 complex enzymatic activity and increased proguanil sensitivity in PfmRPL13 knockdown parasites. *A*, a schematic presentation of the Q cycle in the bc_1 complex, modified from Ref. 33. In the assay, the rate of reduction of oxidized cyt c by reduced Qd catalyzed by the bc_1 complex was measured in mitochondria isolated from *P. falciparum* cultures with a light-scatter rejecting UV/VIS spectrometer (OLIS, Bogart, GA). *B*, the cyt c reduction activity of the bc_1 complex is dramatically reduced in the PfmRPL13 knockdown parasites. In each measurement, activity of the bc_1 complex was determined by recording the absorbance change at 550 nM per microgram of protein in the mix. The bc_1 enzymatic activity of the knockdown cultures was normalized to that of the culture maintained constantly under aTc. Statistical analysis is done by a Student's t test in $n = 3$ experiments. **, $p < 0.001$; *, $p < 0.05$. *C*, hypersensitivity to proguanil in the PfmRPL13 knockdown parasites. The knockdown parasites were grown for three cycles in the absence of aTc before exposure to proguanil. EC_{50} values of proguanil ([μM]) are D10 aTc ON (10.7), D10 aTc OFF (10.6), yDHODH line Atv OFF (6.99), yDHODH line Atv ON (0.11), PfmRPL13 aTc ON (9.56), PfmRPL13 aTc OFF (0.17). *Atv*, atovaquone. Data shown are the mean ± S.D. of three replicates and are representative of $n = 5$ independent experiments.

suggest that proguanil hypersensitivity in the PfmRPL13 knockdown parasites was specifically induced by ablation of PfmRPL13 (see "Discussion").

PfmRPL13 knockdown results in unusual morphological changes in the mitochondria

Next, we used transmission EM (TEM) to assess any morphological alterations in the knockdown parasites. To exclude the possibility that aTc causes changes in parasite morphology, D10 WT parasites were cultured with and without aTc for 2 weeks and their morphologies were examined by TEM ("Materials and methods"). As shown in Fig. S5, with or without aTc, D10 parasites displayed very similar mitochondrial morphologies. Mitochondria in both samples appeared to be circular structures in TEM 2D sections. Because each malaria parasite has just one single tubular mitochondrion (35), it is more likely to obtain cross-sections (circular) than longitudinal sections (tubular) during TEM 2D sample slicing. Mitochondrial morphologies similar to those of D10 were observed in the

PfmRPL13 knockdown parasites maintained continuously in medium with aTc; in each TEM section, there were, again, a small number of circular structures present (Fig. 4). In contrast, when aTc was removed for three cycles, it seemed that more mitochondrial pieces were detected on each TEM section of the knockdown parasite (Fig. 4). In addition, many of the mitochondrial pieces appeared as long tubular structures, sometimes exhibiting branching (Fig. 4). To the best of our knowledge, such elongated and branched mitochondria in trophozoite stages of *P. falciparum* have not been reported previously in TEM studies in the literature. In all, these data revealed interesting morphological changes in parasite mitochondria when PfmRPL13 expression was genetically diminished.

Efforts to rescue PfmRPL13 knockdown parasites grown in the absence of aTc

To gain an understanding of the mechanisms that led to parasite demise when PfmRPL13 was knocked down, we
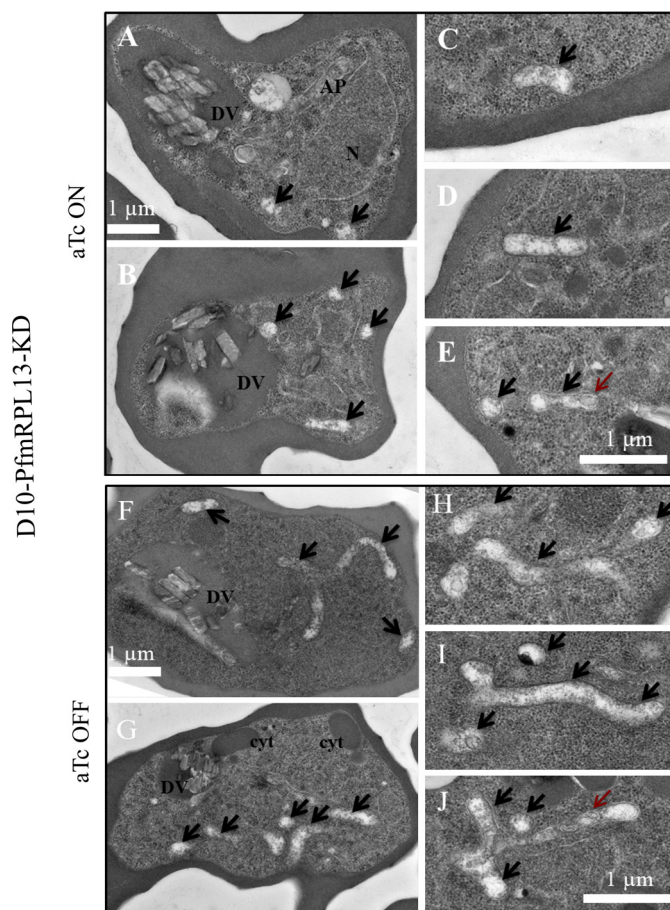
Figure 4. Morphological changes of mitochondria in the PfmRPL13 knockdown parasites maintained with or without aTc under transmission EM. *A–E*, TEM images of PfmRPL13 knockdown parasites maintained constantly under aTc. *DV*, digestive vacuole. *AP*, apicoplast. *N*, nucleus. *F–J*, TEM images of PfmRPL13 knockdown parasites grown without aTc for three cycles. *DV*, digestive vacuole. *Cyt*, cytostome. *Black arrows* indicate mitochondrial sections. *Red arrows* indicate internal membranes within the mitochondrial matrix. Each panel shows either an entire (*A*, *B*, *F*, *G*) or a partial (*C–E*, *H–J*) image of TEM.

attempted to rescue the knockdown parasites with three different approaches. Previous studies in *P. falciparum* have shown that mtETC inhibition by atovaquone can be partially rescued with addition of ubiquinone analogs such as decylubiquinone (Qd) (36). As shown in Fig. 5*A*, however, addition of Qd (50 μM) failed to restore growth of D10-PfmRPL13-KD parasites when aTc had been removed, suggesting that mtETC defects caused by PfmRPL13 knockdown could not be chemically rescued by Qd. Because inhibition of the mtETC by atovaquone can be fully suppressed by expression of a yeast DHODH gene (23), we hypothesized that provision of the yDHODH gene in the knockdown parasites might overcome mtETC defects caused by PfmRPL13 disruption. We then performed a second transfection of the knockdown parasites with an episomal plasmid carrying yDHODH-GFP, resulting in the double transgenic line D10-PfmRPL13-KD-yDHODH-GFP ("Materials and methods"). Expression of the fused yDHODH-GFP protein was confirmed with a fluorescence microscope and Western blotting (data not shown). As shown in Fig. 5*B*, in the absence of aTc, the double transgenic line displayed moderate growth in the first four cycles (short term) but still succumbed to death signifi-

cantly after five cycles or longer without aTc (long term). These data suggested that, in the long term, yDHODH expression still failed to rescue mtETC defects resulting from PfmRPL13 ablation. We then complemented D10-PfmRPL13-KD with an episomal PfmRPL13 tagged with 3Myc, resulting in another double transgenic line, D10-PfmRPL13-KD-RL13Myc ("Materials and methods"). Expression of PfmRPL13Myc was confirmed by Western blotting in the double transgenic line maintained with or without aTc for four cycles (data not shown). As shown in Fig. 5*C*, D10-PfmRPL13-KD-RL13Myc grew equally well in the presence or absence of aTc for a long term. To verify aptamer copy number in the endogenous PfmRPL13 locus of the double transgenic line, D10-PfmRPL13-KD-RL13Myc, we checked its 5′ integration site by PCR and sequencing and eight aptamer copies were still intact (data not shown). Therefore, in the absence of aTc, the endogenous PfmRPL13 was not translated but the double transgenic line was sustained by the episomal expression of PfmRPL13 to maintain growth. Clearly, genetic ablation of PfmRPL13 in the parasite was only rescued with provision of complementing episomal PfmRPL13.

Discussion

With the recent decline in the efficacy of artemisinin-based combination therapies (37), there is an urgent need to discover new antimalarial drugs. The mtETC of the parasite is absolutely essential throughout its complex life cycle. The mtETC is critical both to sustain the essential pyrimidine biosynthesis pathway (23) and to maintain the mitochondrial membrane potential (38). The malarial mtETC has been the focus of many endeavors seeking novel antimalarial drugs (39), yet the structure and function of mitochondrial ribosomes (mitoribosomes), which translate critical protein subunits of the mtETC, remain entirely uncharacterized. In this study, we found that one mitochondrial ribosomal large subunit protein L13 (PfmRPL13) was localized to the mitochondrion (Fig. 1) and was essential for growth of asexual blood stage parasites (Fig. 2). Knockdown of PfmRPL13 resulted in a series of adverse events in the parasite, including loss of $\Delta\psi_m$ (Fig. 2*F*), mtETC deficiency (Fig. 3*B*), and hypersensitivity to proguanil (Fig. 3*C*). Remarkably, PfmRPL13 knockdown also led to unusual mitochondrial morphologies (Fig. 4). For the first time, we provided direct evidence that mitoribosomes are essential in asexual blood stages of malaria parasites. Our genetically tagged parasite line will also be a good tool to study structural and functional aspects of mitoribosomes in the future.

The origin of all eukaryotic mitochondria can be traced back to the integration of an α-protobacterium into the proto-eukaryote ancestor (5, 40). From this single symbiotic event, the common ancestor of all eukaryotic organisms has evolved into the myriad extant cells and organisms with many distinct morphologies and functions that allow survival in drastically different environmental milieus. Needless to say, mitochondria are key players in this ongoing evolutionary adaptation, because they are critical for maintaining cellular bioenergetics, redox balance, signaling, and even life and death decisions (41). However, in apicomplexan parasites, which cause numerous diseases in human and livestock, the mitochondrion has been streamlined by loss of many functions that are important in
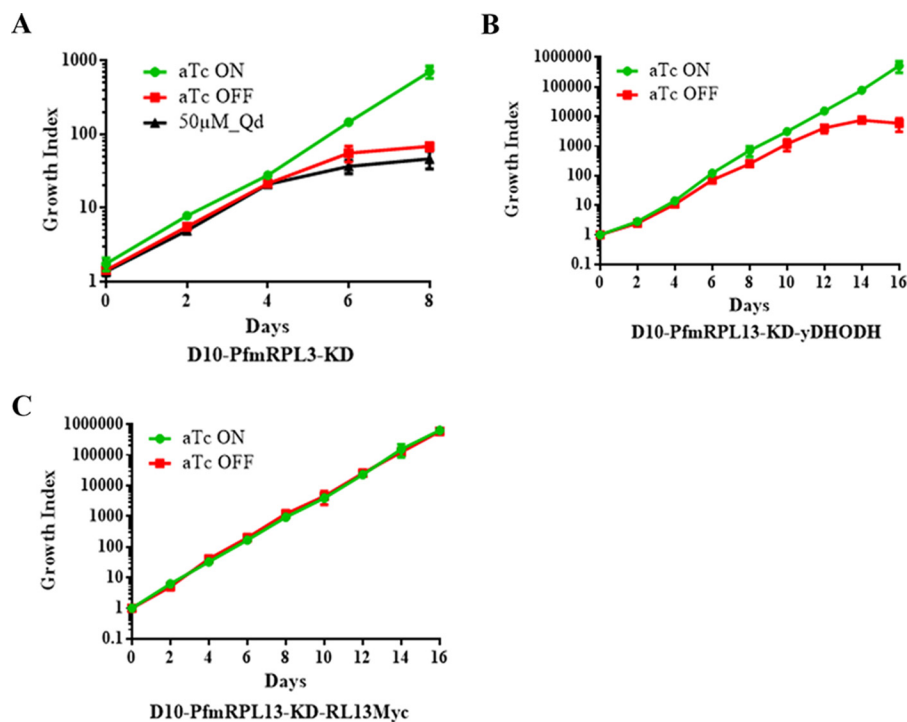
Figure 5. Efforts to rescue growth of the PfmRPL13 knockdown line in the absence of aTc via three approaches. *A*, Qd was unable to rescue growth of the knockdown parasites in the absence of aTc. *B*, provision of episomal copies of yDHODH in the knockdown parasites failed to fully rescue growth without aTc over the long term. *C*, supplementing the knockdown parasites with episomal copies of PfmRPL13–3Myc successfully rescued growth in the absence of aTc. For all conditions, parasitemia and growth index were defined using the same method as descried in Fig. 2C. Data shown are the mean ± S.D. of *n* = 3 biological replicates.

mammalian mitochondria, for example, fatty acid catabolism, amino acid degradation, steroid biosynthesis, and initiation of apoptosis (35). Nevertheless, the mitochondrion is still absolutely essential in every stage of the parasite's life cycle (39). Even *Cryptosporidium,* which has lost the mitochondrial genome, has a mitosome (mitochondrion derivative organelle) that harbors at least one essential biochemical pathway—iron-sulfur cluster biogenesis (8, 42). To maintain protein import and critical biochemical pathways, mitochondria and mitochondrion-related organelles require an electrochemical proton gradient (composed of $\Delta pH + \Delta\psi_m$) across the mitochondrial inner membrane. In malaria parasites, the primary mechanism to sustain $\Delta\psi_m$, the principle component of the proton gradient, is fulfilled by the mtETC (24, 38). Whereas most mtETC proteins are nuclear-encoded and imported into the mitochondrion, three core components are encoded on the 6 kb mtDNA: cyt *b*, COXI, and COXIII. The mitochondrial ribosomes and protein translation system are therefore critical to produce these three mtETC components. In this study, we have shown that PfmRPL13 ablation in *P. falciparum* results in mtETC deficiency (Fig. 3*B*), which leads to the loss of $\Delta\psi_m$ (Fig. 2*F*) and parasite death (Fig. 2*C*). For the first time, we have provided direct evidence that mitochondrial ribosomes are essential in malaria parasites. It is likely that a domino effect follows PfmRPL13 ablation: 1) reduced translation efficiency in mitochondrial ribosomes; 2) shortage of cyt *b*, COXI, and COXIII proteins; 3) failure to assemble functional mtETC complexes; 4) significant reduction of $\Delta\psi_m$; 5) inability to complete pyrimidine biosynthesis, and 6) ultimately parasite death. In the future, we plan to further characterize PfmRPL13 knockdown

parasites to better understand the detailed mechanisms leading to parasite collapse.

One proposed alternative pathway to maintain $\Delta\psi_m$ in malaria parasites is rotation of the F_0F_1 ATP synthase complex (Complex V) in the reverse direction, hydrolyzing ATP (-4 charge) to ADP (-3 charge) (23). One ADP (in the matrix) is then exchanged with one cytosolic ATP, moving one net negative charge across the mitochondrial inner membrane. In addition, ATP hydrolysis by intact coupled Complex V results in the extrusion of protons across the membrane in the opposite direction, providing a further contribution to $\Delta\psi_m$. In the yDHODH transgenic parasites, $\Delta\psi_m$ remained substantially intact even after a complete inhibition of the mtETC by atovaquone, but was rapidly disrupted when proguanil was added subsequently (23). The synergistic effect of atovaquone and proguanil in collapsing $\Delta\psi_m$ suggests that proguanil disrupts the alternative $\Delta\psi_m$ pathway that is likely maintained by Complex V. Remarkably, PfmRPL13 knockdown parasites exhibited proguanil hypersensitivity to a similar degree as yDHODH transgenic parasites under atovaquone inhibition (Fig. 3*C*). These results suggest that PfmRPL13 knockdown caused a severe defect in the mtETC, which rendered parasites reliant on the alternative pathway (proguanil-sensitive) to maintain $\Delta\psi_m$.

Ablation of PfmRPL13 resulted in a significant morphological change in the parasite mitochondria (Fig. 4). It has been well known that the mitochondrion of *P. falciparum* in the asexual blood stages is a tubular structure with very few or no cristae on the inner membrane (35). However, in our PfmRPL13 knockdown parasites, many long tubular and even branched mitochondria were observed in the TEM 2D sections, although they

still remained cristae-deficient (Fig. 4). The mechanisms that led to these unusual morphological changes in the mitochondria of knockdown parasites remain unknown at present. Because there is only one mitochondrion per parasite, it appears that the mitochondrion of the knockdown parasite has undergone a tremendous "growth" in mass and volume. We speculate that mtETC deficiency and/or other mitochondrial defects that result from PfmRPL13 ablation may have triggered a mitochondrial biogenesis pathway(s) to compensate for the loss of mitochondrial components or functions. On the other hand, because these are TEM 2D images, the likelihood that the unusual structures were caused by mitochondrial fragmentation cannot be ruled out. Clearly, further investigation is needed to address these hypotheses.

The results of rescue experiments indicate that the mtETC defects caused by PfmRPL13 knockdown cannot be fully released by addition of the yeast DHODH gene (Fig. 5B), even though yeast DHODH completely restored parasite growth under atovaquone inhibition (23). It has been shown that the bc_1 complex of the yDHODH transgenic line remained fully functional (23). It is likely that atovaquone inhibits the electron transfer activity of the bc_1 complex by binding to the Q_o site of cyt b, but leaving the complex physically intact. In our PfmRPL13 knockdown parasites, however, the mtETC defects seem to be more severe. Mitoribosome deficiency caused by PfmRPL13 knockdown would be expected to compromise both the electron transfer activity and the physical integrity of the mtETC. Although the mtETC can be metabolically bypassed by expression of the yDHODH gene (23), the physical components of the mtETC cannot be supplemented by this exogenous gene. In the PfmRPL13 knockdown parasites, it is likely that loss of integrity of mtETC and $\Delta\psi_m$ causes a wide range of detrimental defects in the mitochondrion. For example, the mitochondrial iron–sulfur cluster biogenesis pathway, dependent on a functional $\Delta\psi_m$, will be deprived, which in turn is detrimental to the mitochondrion and the rest of the parasite. Indeed, our knockdown line was only able to be rescued by complementation with episomal expression of PfmRPL13 (Fig. 5C). These data further support that in addition to its enzymatic activities, physical integrity of the mtETC is essential for mitochondrial physiology.

In summary, we provide direct evidence that the mitochondrial ribosomes in the human malaria parasites are essential. Disruption of mitoribosomes by ablation of a critical protein subunit causes a chain of adverse events and eventual parasite demise. Our data highlight the significance of the mitochondrial protein translation machinery, which is evidently critical to sustain mitochondrial function, structure, and physiology.

Experimental procedures

Plasmid construction

For localization studies, the coding region of *P. falciparum* mitochondrial ribosomal subunit L13 (PfmRPL13, PF3D7_0214200) was cloned into the pLNmRL2 vectors, bearing either a 3HA or GFP tag (43). For CRISPR/Cas9-mediated knockout studies, two homologous regions and one gRNA of PfmRPL13 were cloned into the pL6 vector, which was kindly provided by Dr. Lopez-Rubio (44). The type II *Streptococcus pyogenes* Cas9 was encoded in the pUF1-Cas9 vector (44). For CRISPR/Cas9-mediated knockdown studies, the TetR-DOZI-aptamer system was utilized, which was kindly provided by Dr. Jacquin Niles (30). The original pMG75-ATP4-aptamer vector (30) was reconstructed to remove the attP sites and to replace the single HA tag with a triple HA tag. The pAll-In-One (pAIO) pre-gRNA vector was kindly provided by Dr. Spillman and Dr. Beck (31), which contained Cas9 fused with yDHODH (23) and elements for expressing a gRNA. For complementation studies, a second transfection was performed in the PfmRPL13 knockdown parasites, introducing episomal plasmids of yDHODH-GFP (23) or PfmRPL13–3Myc encoded on a vector that had a human dihydrofolate reductase selectable marker. Details for other cloning procedures are available in the supporting information.

Parasite lines, parasite culture, and transfections

See supporting information for details.

Immunofluorescence assay

Parasite samples (50 μl) were prelabeled with 60 nM Mito-Tracker Red CMXRos (M7512, Life Technologies by Thermo Fisher Scientific), fixed with 4% formaldehyde/0.0075% glutaraldehyde 1 h at 37 °C, permeabilized with 0.1% Triton X-100/PBS for 10 min, treated with 0.1 mg/ml NaBH$_4$ for 5 min and blocked with 5% BSA/PBS before primary and secondary antibody incubations. The HA probe (sc-7392, Santa Cruz Biotechnology) and an Alexa Fluor 488 conjugated anti-mouse secondary antibody (A-21141, Life Technologies by Thermo Fisher Scientific) were used at 1:350 dilution for overnight at 4°. All other steps followed the published protocol (43). The parasites were visualized with an Olympus epifluorescence microscope and images were processed using SlideBook software.

Western blotting

See supporting information for details.

Parasite growth curves and knockdown experiment

Parasite cultures were tightly synchronized with several rounds of alanine treatment (0.5 M alanine/10 mM HEPES, pH 7.6) and trophozoite/schizont stages were isolated using a Percoll gradient (89428−524, GE Healthcare Life Sciences). The highly enriched parasites were thoroughly washed with medium and inoculated into new cultures with each 10 μl parasitized pellet diluted in 10 ml medium containing 1 ml blood. Cultures were maintained in the presence and absence of 250 nM anhydrotetracycline (Millipore Sigma) and were split 1:5 every 2 days. At each split, samples were collected for thin blood smears and protein analysis by Western blotting. Parasitemia was determined by counting at least 1000 RBCs under a Leica light microscope.

MitoTracker staining and quantification

The knockdown experiment was set up as described above. In every 2 days, aliquots of parasitized RBCs (~10 μl pellet)

were taken from cultures maintained with or without aTc, re-suspended in 200 μl medium containing 10 nM MitoTracker Red CMXRos and incubated for 30 min. The parasites were washed three times with 1× PBS, re-suspended in a small volume of medium (~15 μl) and visualized under an Olympus epifluorescence microscope. For each condition, a total of 200 or more parasites were examined within 15 min.

Mitochondrion preparation (Mito Prep)

Mitochondria of *P. falciparum* cultures were isolated according to a published protocol (45). Briefly, parasites were tightly synchronized and expanded to a large volume (~2 liters). Cultures were harvested at late trophozoite stage and lysed with 0.05% saponin. The pellet was washed, re-suspended in a MESH buffer and disrupted using a N_2 cavitation bomb (45). The cell debris was removed by a low speed centrifugation and the supernatant was passed through a MACS Cell Separation Column (Miltenyi Biotec) at 4 °C. The eluted material was pelleted by centrifugation, aliquoted, and stored at −80 °C. Details are listed in the supporting information.

bc₁ complex enzymatic activity measurement

Cytochrome c reductase activity was assayed by a minor modification of published methods (45, 46). The assay was performed at 35 °C in a stirred cuvette with a total volume of 300 μl, which contained 5 μl Mito Prep sample, 100 μM decylubiquinol, 100 μM horse heart cytochrome c (Millipore Sigma), 0.1 mg/ml n-Docecyl β-D-Maltoside, 60 mM HEPES, pH 7.4, 10 mM sodium malonate, 1 mM EDTA, and 2 mM KCN. The reduction of cyt c was recorded at 550 nm with a CLARiTY VF integrating spectrophotometer (OLIS, Bogart, GA). The short chain ubiquinol analog decylubiquinol was prepared by reducing decylubiquinone in DMSO with sodium borohydride and acidifying the mixture with concentrated HCl. Aliquots were stored under argon at −80 °C. Protein concentration of Mito Prep samples was determined by a Bio-Rad colorimetric assay using a spectrometer (Spectronic Genesys 5) at the wavelength of 595 nM.

[³H]Hypoxanthine growth inhibition assay

Growth inhibition assays using [³H]hypoxanthine incorporation were performed in 96-well plates as described previously (36), and data were analyzed by GraphPad Prism 6. See the supporting information for details.

Magnetic enrichment of parasites and transmission EM

aTc was removed from PfmRPL13 knockdown parasites for three intraerythrocytic cycles. Parasites were enriched by a MACS Cell Separation Column in a magnetic apparatus. See the supporting information for other details.

References

1. World Health Organization (2017) World malaria report 2017. WHO Publications, Geneva, Switzerland
2. Gardner, M. J., Hall, N., Fung, E., White, O., Berriman, M., Hyman, R. W., Carlton, J. M., Pain, A., Nelson, K. E., Bowman, S., Paulsen, I. T., James, K., Eisen, J. A., Rutherford, K., Salzberg, S. L., *et al.* (2002) Genome sequence of the human malaria parasite *Plasmodium falciparum*. *Nature* **419,** 498–511 CrossRef Medline
3. Wilson, R. J., Denny, P. W., Preiser, P. R., Rangachari, K., Roberts, K., Roy, A., Whyte, A., Strath, M., Moore, D. J., Moore, P. W., and Williamson, D. H. (1996) Complete gene map of the plastid-like DNA of the malaria parasite *Plasmodium falciparum*. *J. Mol. Biol.* **261,** 155–172 CrossRef Medline
4. Goodman, C. D., and McFadden, G. I. (2014) Ycf93 (Orf105), a small apicoplast-encoded membrane protein in the relict plastid of the malaria parasite *Plasmodium falciparum* that is conserved in Apicomplexa. *PLoS One* **9,** e91178 CrossRef Medline
5. Gray, M. W. (2014) The pre-endosymbiont hypothesis: A new perspective on the origin and evolution of mitochondria. *Cold Spring Harb. Perspect. Biol.* **6,** a016097 CrossRef Medline
6. Vaidya, A. B., Akella, R., and Suplick, K. (1989) Sequences similar to genes for two mitochondrial proteins and portions of ribosomal RNA in tandemly arrayed 6-kilobase-pair DNA of a malarial parasite. *Mol. Biochem. Parasitol.* **35,** 97–107 CrossRef Medline
7. Hikosaka, K., Kita, K., and Tanabe, K. (2013) Diversity of mitochondrial genome structure in the phylum Apicomplexa. *Mol. Biochem. Parasitol.* **188,** 26–33 CrossRef Medline
8. Puiu, D., Enomoto, S., Buck, G. A., Abrahamsen, M. S., and Kissinger, J. C. (2004) CryptoDB: the Cryptosporidium genome resource. *Nucleic Acids Res.* **32,** D329–D331 CrossRef Medline
9. Suplick, K., Akella, R., Saul, A., and Vaidya, A. B. (1988) Molecular cloning and partial sequence of a 5.8 kilobase pair repetitive DNA from *Plasmodium falciparum*. *Mol. Biochem. Parasitol.* **30,** 289–290 CrossRef Medline
10. Feagin, J. E. (1992) The 6-kb element of *Plasmodium falciparum* encodes mitochondrial cytochrome genes. *Mol. Biochem. Parasitol.* **52,** 145–148 CrossRef Medline
11. Feagin, J. E., Werner, E., Gardner, M. J., Williamson, D. H., and Wilson, R. J. (1992) Homologies between the contiguous and fragmented rRNAs of the two *Plasmodium falciparum* extrachromosomal DNAs are limited to core sequences. *Nucleic Acids Res.* **20,** 879–887 CrossRef Medline
12. Suplick, K., Morrisey, J., and Vaidya, A. B. (1990) Complex transcription from the extrachromosomal DNA encoding mitochondrial functions of *Plasmodium yoelii*. *Mol. Cell. Biol.* **10,** 6381–6388 CrossRef Medline
13. Feagin, J. E., Harrell, M. I., Lee, J. C., Coe, K. J., Sands, B. H., Cannone, J. J., Tami, G., Schnare, M. N., and Gutell, R. R. (2012) The fragmented mitochondrial ribosomal RNAs of *Plasmodium falciparum*. *PLoS One* **7,** e38320 CrossRef Medline
14. Sharma, A., and Sharma, A. (2015) *Plasmodium falciparum* mitochondria import tRNAs along with an active phenylalanyl-tRNA synthetase. *Biochem. J.* **465,** 459–469 CrossRef Medline
15. Aikawa, M. (1966) The fine structure of the erythrocytic stages of three avian malarial parasites, *Plasmodium fallax*, *P. lophurae*, and *P. cathemerium*. *Am. J. Trop. Med. Hyg.* **15,** 449–471 CrossRef Medline

ASBMB

16. Wong, W., Bai, X. C., Brown, A., Fernandez, I. S., Hanssen, E., Condron, M., Tan, Y. H., Baum, J., and Scheres, S. H. (2014) Cryo-EM structure of the *Plasmodium falciparum* 80S ribosome bound to the anti-protozoan drug emetine. *Elife* **3,** 03080 CrossRef Medline

17. Sun, M., Li, W., Blomqvist, K., Das, S., Hashem, Y., Dvorin, J. D., and Frank, J. (2015) Dynamical features of the *Plasmodium falciparum* ribosome during translation. *Nucleic Acids Res.* **43,** 10515–10524 CrossRef Medline

18. Gupta, A., Shah, P., Haider, A., Gupta, K., Siddiqi, M. I., Ralph, S. A., and Habib, S. (2014) Reduced ribosomes of the apicoplast and mitochondrion of *Plasmodium* spp., and predicted interactions with antibiotics. *Open Biol.* **4,** 140045 CrossRef Medline

19. Chaubey, S., Kumar, A., Singh, D., and Habib, S. (2005) The apicoplast of *Plasmodium falciparum* is translationally active. *Mol. Microbiol.* **56,** 81–89 CrossRef Medline

20. Goodman, C. D., Pasaje, C. F. A., Kennedy, K., McFadden, G. I., and Ralph, S. A. (2016) Targeting protein translation in organelles of the Apicomplexa. *Trends Parasitol.* **32,** 953–965 CrossRef Medline

21. Dahl, E. L., and Rosenthal, P. J. (2007) Multiple antibiotics exert delayed effects against the *Plasmodium falciparum* apicoplast. *Antimicrob. Agents Chemother.* **51,** 3485–3490 CrossRef Medline

22. Camps, M., Arrizabalaga, G., and Boothroyd, J. (2002) An rRNA mutation identifies the apicoplast as the target for clindamycin in *Toxoplasma gondii. Mol. Microbiol.* **43,** 1309–1318 CrossRef Medline

23. Painter, H. J., Morrisey, J. M., Mather, M. W., and Vaidya, A. B. (2007) Specific role of mitochondrial electron transport in blood-stage *Plasmodium falciparum. Nature* **446,** 88–91 CrossRef Medline

24. Fry, M., and Pudney, M. (1992) Site of action of the antimalarial hydroxynaphthoquinone, 2-[trans-4-(4′-chlorophenyl) cyclohexyl]-3-hydroxy-1,4-naphthoquinone (566C80). *Biochem. Pharmacol.* **43,** 1545–1553 CrossRef Medline

25. Vaidya, A. B., and Mather, M. W. (2000) Atovaquone resistance in malaria parasites. *Drug Resist. Updates* **3,** 283–287 CrossRef Medline

26. Timsit, Y., Acosta, Z., Allemand, F., Chiaruttini, C., and Springer, M. (2009) The role of disordered ribosomal protein extensions in the early steps of eubacterial 50S ribosomal subunit assembly. *Int. J. Mol. Sci.* **10,** 817–834 CrossRef Medline

27. Khaitovich, P., Mankin, A. S., Green, R., Lancaster, L., and Noller, H. F. (1999) Characterization of functionally active subribosomal particles from *Thermus aquaticus. Proc. Natl. Acad. Sci. U.S.A.* **96,** 85–90 CrossRef Medline

28. Nkrumah, L. J., Muhle, R. A., Moura, P. A., Ghosh, P., Hatfull, G. F., Jacobs, W. R., Jr., and Fidock, D. A. (2006) Efficient site-specific integration in *Plasmodium falciparum* chromosomes mediated by mycobacteriophage Bxb1 integrase. *Nat. Methods* **3,** 615–621 CrossRef Medline

29. Smits, P., Smeitink, J. A., van den Heuvel, L. P., Huynen, M. A., and Ettema, T. J. (2007) Reconstructing the evolution of the mitochondrial ribosomal proteome. *Nucleic Acids Res.* **35,** 4686–4703 CrossRef Medline

30. Ganesan, S. M., Falla, A., Goldfless, S. J., Nasamu, A. S., and Niles, J. C. (2016) Synthetic RNA-protein modules integrated with native translation mechanisms to control gene expression in malaria parasites. *Nat. Commun.* **7,** 10727 CrossRef Medline

31. Spillman, N. J., Beck, J. R., Ganesan, S. M., Niles, J. C., and Goldberg, D. E. (2017) The chaperonin TRiC forms an oligomeric complex in the malaria parasite cytosol. *Cell Microbiol.* **19,** 12719 CrossRef Medline

32. Bushell, E., Gomes, A. R., Sanderson, T., Anar, B., Girling, G., Herd, C., Metcalf, T., Modrzynska, K., Schwach, F., Martin, R. E., Mather, M. W., McFadden, G. I., Parts, L., Rutledge, G. G., Vaidya, A. B., Wengelnik, K., Rayner, J. C., and Billker, O. (2017) Functional profiling of a *Plasmodium* genome reveals an abundance of essential genes. *Cell* **170,** 260–272.e8 CrossRef Medline

33. Hunte, C., Palsdottir, H., and Trumpower, B. L. (2003) Proton motive pathways and mechanisms in the cytochrome bc1 complex. *FEBS Lett.* **545,** 39–46 CrossRef Medline

34. Das, S., Bhatanagar, S., Morrisey, J. M., Daly, T. M., Burns, J. M., Jr., Coppens, I., and Vaidya, A. B. (2016) Na+ influx induced by new antimalarials causes rapid alterations in the cholesterol content and morphology of *Plasmodium falciparum. PLoS Pathog.* **12,** e1005647 CrossRef Medline

35. Vaidya, A. B., and Mather, M. W. (2009) Mitochondrial evolution and functions in malaria parasites. *Annu Rev. Microbiol.* **63,** 249–267 CrossRef Medline

36. Ke, H., Morrisey, J. M., Ganesan, S. M., Painter, H. J., Mather, M. W., and Vaidya, A. B. (2011) Variation among *Plasmodium falciparum* strains in their reliance on mitochondrial electron transport chain function. *Eukaryot. Cell* **10,** 1053–1061 CrossRef Medline

37. Ashley, E. A., Dhorda, M., Fairhurst, R. M., Amaratunga, C., Lim, P., Suon, S., Sreng, S., Anderson, J. M., Mao, S., Sam, B., Sopha, C., Chuor, C. M., Nguon, C., Sovannaroth, S., Pukrittayakamee, S., *et al.* (2014) Spread of artemisinin resistance in *Plasmodium falciparum* malaria. *N. Engl. J. Med.* **371,** 411–423 CrossRef Medline

38. Srivastava, I. K., Rottenberg, H., and Vaidya, A. B. (1997) Atovaquone, a broad spectrum antiparasitic drug, collapses mitochondrial membrane potential in a malarial parasite. *J. Biol. Chem.* **272,** 3961–3966 CrossRef Medline

39. Ke, H., and Mather, M. (2017) +Targeting mitochondrial functions as antimalarial regime, what is next? *Curr. Clin. Micro. Rpt.* **4,** 175–191 CrossRef

40. Burger, G., Gray, M. W., Forget, L., and Lang, B. F. (2013) Strikingly bacteria-like and gene-rich mitochondrial genomes throughout jakobid protists. *Genome Biol. Evol.* **5,** 418–438 CrossRef Medline

41. Vafai, S. B., and Mootha, V. K. (2012) Mitochondrial disorders as windows into an ancient organelle. *Nature* **491,** 374–383 CrossRef Medline

42. Lill, R., Srinivasan, V., and Mühlenhoff, U. (2014) The role of mitochondria in cytosolic-nuclear iron-sulfur protein biogenesis and in cellular iron regulation. *Curr. Opin. Microbiol.* **22,** 111–119 CrossRef Medline

43. Balabaskaran Nina, P., Morrisey, J. M., Ganesan, S. M., Ke, H., Pershing, A. M., Mather, M. W., and Vaidya, A. B. (2011) ATP synthase complex of *Plasmodium falciparum*: Dimeric assembly in mitochondrial membranes and resistance to genetic disruption. *J. Biol. Chem.* **286,** 41312–41322 CrossRef Medline

44. Ghorbal, M., Gorman, M., Macpherson, C. R., Martins, R. M., Scherf, A., and Lopez-Rubio, J. J. (2014) Genome editing in the human malaria parasite *Plasmodium falciparum* using the CRISPR-Cas9 system. *Nat. Biotechnol.* **32,** 819–821 CrossRef Medline

45. Mather, M. W., Morrisey, J. M., and Vaidya, A. B. (2010) Hemozoin-free *Plasmodium falciparum* mitochondria for physiological and drug susceptibility studies. *Mol. Biochem. Parasitol.* **174,** 150–153 CrossRef Medline

46. Trumpower, B. L., and Edwards, C. A. (1979) Purification of a reconstitutively active iron-sulfur protein (oxidation factor) from succinate. Cytochrome c reductase complex of bovine heart mitochondria. *J. Biol. Chem.* **254,** 8697–8706 Medline

47. Aurrecoechea, C., Brestelli, J., Brunk, B. P., Dommer, J., Fischer, S., Gajria, B., Gao, X., Gingle, A., Grant, G., Harb, O. S., Heiges, M., Innamorato, F., Iodice, J., Kissinger, J. C., Kraemer, E., *et al.* (2009) PlasmoDB: a functional genomic database for malaria parasites. *Nucleic Acids Res.* **37,** D539–D543 CrossRef Medline

ASBMB

J. Biol. Chem. (2018) 293(21) 8128–8137 **8137**

The mitochondrial ribosomal protein L13 is critical for the structural and functional integrity of the mitochondrion in *Plasmodium falciparum*

Hangjun Ke, Swati Dass, Joanne M. Morrisey, Michael W. Mather and Akhil B. Vaidya

Access the most updated version of this article at doi: 10.1074/jbc.RA118.002552

Alerts:
- When this article is cited
- When a correction for this article is posted

Click here to choose from all of JBC's e-mail alerts

This article cites 46 references, 12 of which can be accessed free at
http://www.jbc.org/content/293/21/8128.full.html#ref-list-1

Supporting Information

The mitochondrial ribosomal protein L13 is critical for the structural and functional integrity of the mitochondrion in *Plasmodium falciparum*

Hangjun Ke[1*], Swati Dass[1], Joanne M. Morrisey[1], Michael W. Mather[1], and Akhil B. Vaidya[1]

[1]From the Center for Molecular Parasitology, Department of Microbiology and Immunology, Drexel University College of Medicine, Philadelphia, PA 19129, USA

Running title: Mitochondrial ribosomal protein L13 in *Plasmodium falciparum*

To whom correspondence should be addressed: Hangjun Ke, Center for Molecular Parasitology, Department of Microbiology and Immunology, Drexel University College of Medicine, 2900 Queen Lane, Philadelphia, PA 19129, USA. Tel.: (215) 991-8448; Fax: (215) 848-2271; E-mail: hk84@drexel.edu

List of Content:

Materials and methods

Table S1

Figure S2

Figure S3

Figure S4

Figure S5

References

Materials and methods

   1. Plasmid construction.

1) The genomic region of the putative *P. falciparum* mitochondrial ribosomal subunit L13 (PfmRPL13, PF3D7_0214200) is 900 bp, which includes one intron of 261 bp from +90 to +350. For localization studies, the coding region of PfmRPL13 was amplified from cDNA of wildtype 3D7 parasites using primers P1 and P2 (Table S1). The PfmRPL13 fragment was then cloned into the pLNmRL2 vector (1) via *Avr* II and *Bsi*W I restriction endonucleases to yield a copy of PfmRPL13 tagged with 3HA or GFP at the C-termini, namely pLN-PfmRPL13-3HA or pLN-PfmRPL13-GFP, respectively. The pLNmRL2 vectors with 3HA or GFP tags were derived from the original pLN-ENR-GFP plasmid generated by Nkrumah *et al.* (2).

2) The pL6 and pUF1-Cas9 vectors were kindly provided by Dr. Lopez-Rubio (3). The pL6 plasmid bears a cassette for expressing a single guide RNA (sgRNA), namely the *P. falciparum* U6 small nuclear RNA regulatory system (3). To perform knockout studies mediated with CRISPR/Cas9, two homologous regions of PfmRPL13, 5HR and 3HR, and a gRNA were cloned into the pL6 vector. The homologous regions were amplified from 3D7 genomic DNA using P3+P4 (5HR) and P5+P6 (3HR) primer pairs (Table S1) and were sequentially cloned into the pL6 vector, resulting in a primitive PfmRPL13 knockout construct without gRNA (pL6-PfmRPL13-pKO). The 5HR is a 608 bp fragment from -529 to +79 of the PfmRPL13 genomic region and was cloned via *Sac* II and *Afl* II. The 3HR is a 681 bp fragment from positions +388 to +1068 and was cloned via *Eco*R I and *Nco* I. To search for the best gRNA for CRISPR/Cas9 mediated knockout, a fragment between the two homologous regions (308 bp) was analyzed by the Eukaryotic Pathogen CRISPR guide RNA Design Tool (http://grna.ctegd.uga.edu/). From all potential hits, the best available gRNA was chosen based on its high efficiency score and zero off-target matches. This gRNA was named RL13KO_gRNA, and the sequence was 5'-GGCATATTCTTCTTTAAAAA(TGG)-3'. It was cloned into the pL6-PfmRPL13-pKO vector via InFusion cloning according to the manufacture's guidance (Clontech® Laboratories, Inc.). Briefly, the

pL6-PfmRPL13-pKO vector was linearized with *Btg*Z I. We synthesized a 60 bp oligo that harbors a 20

bp sequence homologous to the segment immediately upstream of the *Btg*Z I site of the pL6-PfmRPL13-

pKO vector, a 20 bp RL13KO_gRNA sequence and another 20 bp sequence homologous to the segment

immediately downstream of the *Btg*Z I site of the vector. The reverse complement strand (60 bp) was also

synthesized. These two 60 bp oligoes, RL13-oligo1 (P7) and RL13-oligo2 (P8), were then mixed in a 1:1

mixture of Buffer 2 and Buffer 4 (New England Biolabs®, Inc.), heated at 95 ℃ for 5 min and gradually

cooled down to room temperature. The annealed oligoes and the linearized pL6-PfmRPL13-pKO vector

were then joined by InFusion cloning to yield the pL6-PfmRPL13-KO vector for knockout studies. The

N20 of RL13KO_gRNA (P9) and a vector primer from the pL6 vector (P10) were used to diagnose

positive clones. Another oligo (P11), 71bp downstream of *Btg*Z I site, was used to sequence the cloned

gRNA.

3) To do knockdown studies, we utilized the TetR-DOZI-aptamer system, recently developed and kindly

provided by Dr. Jacquin Niles' group at MIT (4). Based on this system (4), Spillman and Beck *et al.*

developed a double crossover integration strategy to insert aptamer copies mediated with the

CRISPR/Cas9 system (5). They developed a pAll-In-One (pAIO) vector which contained Cas9 infused

with the yDHODH gene (6) and elements for expressing a gRNA (5). Dr. Spillman and Dr. Beck kindly

provided us with this all-in-one vector. We then cloned two gRNAs of PfmRPL13 into the pAIO vector

via InFusion cloning as described above, generating pAIO-RL13-gRNA1 and pAIO-RL13-gRNA2,

respectively. These two gRNAs of PfmRPL13 were located immediately upstream and downstream of the

stop codon of PfmRPL13, respectively. The oligoes used for making these gRNA constructs and

diagnostic PCRs were listed in Table S1 from P12 to P17.

The original pMG75-ATP4 vector (4) contains two attP sites for quick site specific genome insertions via

the attBXattP system in attB positive strains (2). This facilitated a quick knockdown using the TetR-

DOZI-aptamer system at an ectopical site, but not at the endogenous locus. An attP site is not required for

endogenous gene insertion. To remove two attP sites from the pMG75-ATP4 vector, pMG75-ATP4 was

digested with *Sal* I and *Not* I, treated with Klenow, and re-ligated by T4 DNA ligase. Removal of two attP

sites from pMG75-ATP4 was confirmed by PCR and sequencing using P18+P19 primers. Interestingly,

during this process, 2 aptamer copies were lost (confirmed by PCR analysis and sequencing (P20+P21)).

Therefore, this process resulted in a modified vector with 8 copies of aptamers, pMG75noP_ATP4_8apt.

As the original vector, this vector contains a single copy of MYC tag and a single copy of HA tag. To

increase tag affinity, we removed the single epitope tags from pMG75noP_ATP4_8apt and replaced it

with a 3HA.

Next, we cloned two homologous regions (5'HR and3'HR) of PfmRPL13 into the modified vector,

pMG75noP_ATP4_8apt_3HA. The 3'HR of PfmRPL13 (869 bp) was immediately downstream of the

stop codon and was amplified via P22+P23 primers. It was cloned into the vector using *Sac* II and *Bst*E II

sites. The 5'HR of PfmRPL13 was amplified via P24+P25 primers and cloned into the vector bearing

3'HR via *Bst*E II and *Sal* I sites. To avoid repetitive cutting by Cas9 in the transgenic parasites, the

reverse primer (P25) of 5'HR included synonymous mutations within the pAIO-RL13-gRNA1 region.

The pAIO-RL13-gRNA2 was located between the stop codon and 3'HR; therefore no synonymous

mutations were needed. These procedures yielded the vector for double crossover recombination and

knockdown studies, pMG75noP_PfmRPL13_8apt_3HA. The plasmid was linearized with *Eco*R V and

transfected into parasites together with two gRNA constructs, pAIO-RL13-gRNA1 and pAIO-RL13-

gRNA2.

4) For complementation studies in the knockdown parasites, we performed a second transfection by

introducing an extra copy of yDHODH or PfmRPL13, respectively. Since the knockdown parasites

already had bsd (blasticidin deaminase) from pMG75 (resistant to blasticidin) and yDHODH from pUF1

(resistant to DSM1), the hdhfr (human dihydrofolate reductase) marker (resistant to WR99210) was used

for additional transfections. A copy of yDHODH was previously cloned into a pHH vector bearing an

hdhfr cassette (6). In case of PfmRPL13, we started with the pLN-PfmRPL13-3HA construct (described as above) by replacing the bsd marker with hdhfr and changing the 3HA tag to 3Myc. To do that, the pLN-PfmRPL13-3HA plasmid was digested with *Nco* I and *Bpu10* I to release the bsd marker. The hdhfr gene was amplified from pCC1 using primers (P26+P27) which had overlapping regions homologous to the pLN vector. The linearized pLN vector and the hdhfr fragment were annealed by InFusion cloning, resulting in a modified pLN vector with an hdhfr selectable marker, namely pLN-hdhfr-PfmRPL13-3HA. The PfmRPL13-3HA was then removed by digesting the vector with *Avr* II and *Afl* II. A synthetic DNA fragment of PfmRPL13 plus a 3Myc tag was synthesized as a gene block (Genewiz LLC), digested with *Avr* II and *Afl* II, and put into the vector by ligation, yielding the pLN-hdhfr-PfmRPL13-3Myc construct for complementation studies.

All primers and oligoes were purchased from Eurofins Genomics (Table S1). DNA fragments used for cloning were amplified with high fidelity DNA polymerases followed by sequencing confirmation (Genewiz LLC). All restriction endonucleases and DNA modifying enzymes were purchased from New England Biolabs®, Inc. All cloning steps involving pMG75-derived vectors were transformed into stable competent *E. coli* (New England Biolabs®, Inc) and bacteria were grown at 30 °C.

2. Parasite lines, parasite culture, and transfection.

P. falciparum strains used in this study included Dd2attB (2), NF54attB (7), D10 wildtype, and NF54 wildtype. Asexual *P. falciparum* parasites were cultured using RPMI medium supplemented with 0.5% Albumax II (Gibco by Life technologies) under a low oxygen atmosphere (6% O_2, 5% CO_2, 89% N_2), as described previously (8). Human blood (O^+) was purchased from the Interstate Blood Bank in Tennessee. Parasite transfections were performed in cultures with 5% rings using circular template plasmids (50 µg each electroporation) or linearized template plasmids (20-50 µg each electroporation) together with circular gRNA constructs (50 µg for each gRNA in each electroporation). Restriction endonucleases used

to linearize pL6-PfmRPL13-pKO and pMG75noP_ATP4_8apt were *Hinc* II and *Eco*R V, respectively.

Drug selections were added 48 h post electroporation and maintained under the following concentrations: 5 nM WR99210 for hdhfr, 2.5 µg/ml blasticidin for blasticidin deaminase, 1.5 µM DSM1 for yDHODH (yeast dihydroorotate dehydrogenase), 125 µg/ml G418 for the neomycin selectable cassette, 2 µM 5-flurocytosine (5-FC) for FCU gene (yeast cytosine deaminase/uracil phosphoribosyl transferase).

3. Gene knockout approaches.

The CRISPR/Cas9 gene knockout approach was implemented (3) in two wildtype *P. falciparum* lines, D10 and NF54. They were individually transfected with a circular or linearized pL6-PfmRPL13-KO plasmid PfmRPL13 (containing two homologous regions and one gRNA) and pUF1-Cas9. These transfections were selected only with WR99210 for pL6-PfmRPL13-KO vector whereas Cas9 was expressed transiently. In parasite lines transfected with circular pL6-PfmRPL13-KO plasmid which still contains a negative selection marker, namely the FCU gene (the yeast cytosine deaminase and uracil phosphoribosyl transferase), we also performed negative selections with 5-FC in combination with WR99210 directly or after one round of drug off-and-on cycling. We also repeated transfections in D10 and NF54 lines using dual drug selections with WR99210 and DSM1. Since it has not been determined how long Cas9 is needed to obtain a knockout parasite in the literature, DSM1 was administered for one, two or four weeks post transfections along with WR99210.

4. Western blot.

Infected RBCs were treated with 0.05% saponin (MilliporeSigma) in PBS in the presence of 1x protease inhibitor cocktail (MilliporeSigma) and the parasitized pellet was resuspended in 2% SDS/62 mM Tris-HCl (pH 6.8) by repeated pipetting. The lysate was then spun down at 10,000 rpm for 5 min and the supernatant was then processed for SDS-PAGE analysis. Protein transfer, blocking, and other steps followed the standard protocol. The anti-HA primary antibody (sc-7392, Santa Cruz Biotechnology) was

used at 1: 10,000 and an HRP conjugated secondary anti-mouse antibody was used at 1: 10,000. The antibody against *P. falciparum* aldolase (ab38905, Abcam) was served as a positive control (1: 20,000).

5. Mitochondrion preparation (Mito-prep).

Mitochondrial isolation was performed according to a published protocol (9). For aTc plus parasites, cultures were tightly synchronized with alanine and expanded to 1.6-2.4 liters (4-6 T225 flasks). For aTc minus parasites, the culture was first grown under 250 nM aTc up to one T225 flask, and late stages were isolated by a Percoll gradient, as described above. The isolated parasites were washed 3 times with medium, and inoculated into new T225 flasks and maintained under regular RPMI (aTc minus) for 2 cycles or 4 cycles. After the desired growth, the parasites were harvested at trophozoite stages and lysed with 0.05% saponin in AIM buffer (120 mM KCl, 20 mM NaCl, 20 mM glucose, 6 mM HEPES, 6 mM MOPS, 1 mM MgCl2, 0.1 mM EGTA, pH 7.0) and washed three times with cold AIM buffer. The pellet was resuspended in argon deaerated MESH buffer (225 mM mannitol, 75 mM sucrose, 4.3 mM MgCl2, 0.25 mM EGTA, 10 mM HEPES [Tris], 5 mM HEPES [KOH], pH 7.4) containing 10 mM glucose and mitochondrial substrates (5 mM succinate and 5 mM L-malate) in the presence of 1 mM PMSF (Millipore Sigma) and 1 μl per ml fungal protease inhibitor cocktail (MilliporeSigma). The parasite suspension was added into a metal pressure chamber on ice and disrupted by N_2 cavitation, as previously described (9). The unbroken cells and cell debris were removed by centrifugation at 900 $\times g$ for 6 min at 4 °C. The low speed supernatant was passed slowly (~0.2 ml/min) through a MACS CS column (Miltenyi Biotec) prewashed with MSEH buffer in a Vario MACS magnetic separation apparatus (Miltenyi Biotec) to remove most of the hemozoin from the preparation. This step was conducted at 4 °C. The eluted material was pelleted by centrifugation at 23,000 $\times g$ for 20 min at 4 °C. The pellet was suspended in an appropriate volume (~500-1000 μl) of MSEH buffer containing 1.0 mM succinate, aliquoted in 50 μl aliquots, and used for enzymatic assays or stored at -80 °C.

6. ^{3}H-hypoxanthine growth inhibition assay.

Growth inhibition assays using ^{3}H-hypoxanthine incorporation were performed in 96 well plates as previously described (10). For drug assays, mixed stage parasites at 1% parasitemia and 3% hematocrit were exposed to compounds diluted by a serial dilution for 24 h. Then each well was pulsed with 10 μl of 0.5 μCi ^{3}H-hypoxanthine and incubated for another 24 h. Parasites were then lysed by freeze-thawing and nucleic acids were collected onto filters with a cell harvester (Perkin Elmer, MA). The filters were dried and counted with a Topcount scintillation counter (Perkin Elmer, MA) after addition of MicroScint O. For measuring parasite growth under aTc or in the absence of aTc for 1 cycle, parasites with 1% parasitemia and 3% hematocrit were inoculated into 96 well plates. ^{3}H-hypoxanthine was added 24 h later and incubated for another 24 h (in total of 48 h). For measuring growth for 2 cycles, parasites with 0.5% parasitemia and 3% hematocrit were inoculated. ^{3}H-hypoxanthine was added 72 h later and incubated for additional 24 h (in total of 96 h). Other steps followed the procedures described as above. GraphPad Prism 6 was used to graph the data.

7. Magnetic enrichment and transmission electron microscopy.

During knockdown experiments as described above, on day 6, the culture was spun down, re-suspended into 20% hematocrit, and bound to a MACS CS column prewashed with medium in the Vario MACS magnetic separation apparatus. Uninfected RBCs were washed from the CS column and the infected RBCs were harvested by washing the CS column after it was removed from the magnetic field. The enriched parasites, mostly late trophozoite/schizont stages, were washed with 100 mM sodium cacodylate and fixed with 2% paraformaldehyde/2.5% glutaraldehyde/100 mM sodium cacodylate at RT for 1 h. The fixed parasites were washed once with 100 mM sodium cacodylate and shipped to the Molecular Microbiology Imaging Facility at Washington University in St. Louis. Samples were then washed once with 100 mM sodium cacodylate and post-fixed in 1% osmium tetroxide (Polysciences Inc.) for 1 h. Samples were then rinsed extensively in dH$_2$O prior to en bloc staining with 1% aqueous uranyl acetate (Ted Pella Inc.) for 1 h. Following several rinses in dH$_2$O, samples were dehydrated in a graded series of ethanol and embedded in Eponate 12 resin (Ted Pella Inc.). Sections of 95 nm were cut with a

Leica Ultracut UCT ultramicrotome (Leica Microsystems Inc.), stained with uranyl acetate and lead citrate, and viewed on a JEOL 1200 EX Transmission Electron Microscope (JEOL USA Inc.) equipped with an AMT 8 megapixel digital camera and AMT Image Capture Engine V602 software (Advanced Microscopy Techniques).

Table S1. Sequences of primers and oligoes used in this study.

Primer ID	Description	Sequence
P1	RL13-F-BsiWI-AvrII	aTcgtacgcctaggATGATAAGAAGAAGCTTGATTAAATTAG
P2	RL13-R-BsiWI-AflII	GTcgtacgcttaagCAAAATGGTAAAGGTCTTTATATC
P3	RL13-5fF-SacII	ttCCGCGGCAAAAAAGGTCCCGGAGTACA
P4	RL13-5fR-AflII	aaCTTAAGTTGAAAAAGGGTTAATGTGCTG
P5	RL13-3fF-EcoRI	aaGAATTCGTTGATATTTTTTCAGAAGAAC
P6	RL13-3fR-NcoI	aaCCATGGTTTATGTGCTGTGTTATGTTG
P7	RL13-oligo1	CATATTAAGTATATAATATTGGCATATTCTTCTTTAAAAAGTTTTAGAGCTAGAAATAGC
P8	RL13-oligo2	GCTATTTCTAGCTCTAAAACTTTTTAAAGAAGAATATGCCAATATTATATACTTAATATG
P9	RL13KO_gRNAN20	GGCATATTCTTCTTTAAAAA
P10	N20CheckR	ATATGAATTACAAATATTGCATAAAGA
P11	gRNArevo	TAGGAAATAATAAAAaagcacc
P12	RL13-oligo5	CATATTAAGTATATAATATTGATATTGTTACAAAATGGTAAGTTTTAGAGCTAGAAATAGC
P13	RL13-oligo6	GCTATTTCTAGCTCTAAAACTTACCATTTTGTAACAATATCAATATTATATACTTAATATG
P14	RL13apt_gRNA1N20	ATATTGTTACAAAATGGTAA

P15	RL13-oligo7	CATATTAAGTATATAATATTGTAACACAGCACATAAACATTGTT TTAGAGCTAGAAATAGC
P16	RL13-oligo8	GCTATTTCTAGCTCTAAAACAATGTTTATGTGCTGTGTTACAAT ATTATATACTTAATATG
P17	RL13apt_gRNA2 N20	TAACACAGCACATAAACATT
P18	revattPF	GTTAATTCATCAAATAGCATGCCTG
P19	revattPR	AGCTGGCACGACAGGTTTCC
P20	pMG75AptF	CACCAGGTGATTATAAAGATGATGATG
P21	pMG75AptR	GTAGACCCCATTGTGAGTAC
P22	RL13_3UTRF	aTcCGCGGtCTTAAGCATTAGTCCACTTTTTTAATATAACATATT ATGCAC
P23	RL13_3UTRR	ctGGTTACCaTcATTTTGATATGTACTTTATACTTGGC
P24	RL13_5HRF	ctGGTTACCtaGATATCaaCCGCGGataTcAGCACATTAACCCTTTTT C
P25	RL13_5HRR	ATGTCGACCTGCAGTAATATTGTGAATGTCTTTATATCTTGCTG CTCTTCC
P26	hdhfrFToBSD	GCTTATATATATACACACACCTAAAACTTACAAACCGGTccatgga aaaATGCATGGTTCGCTAAACTGCATC
P27	hdhfrRToBSD	AATCTATTATTAAATAAATTTAATGGGGTACCTTAGCTCCGGAt TAATCATTCTTCTCATATACTTCAAATTTGTAC

Figure S1A

```
HUMAN/1-178     ------------------------------------------------------------------------------------------------------------
MOUSE/1-178     ------------------------------------------------------------------------------------------------------------
DANre/1-179     ------------------------------------------------------------------------------------------------------------
DROme/1-178     ------------------------------------------------------------------------------------------------------------
ANIga/1-177     ------------------------------------------------------------------------------------------------------------
CAEel/1-205   1 M------------------------------------------------------------------------------------------------------- 1
YEAST/1-163     ------------------------------------------------------------------------------------------------------------
NEUcr/1-183     ------------------------------------------------------------------------------------------------------------
DICdi/1-227     ------------------------------------------------------------------------------------------------------------
ESCco/1-142     ------------------------------------------------------------------------------------------------------------
BRUsu/1-154     ------------------------------------------------------------------------------------------------------------
RICpr/1-155     ------------------------------------------------------------------------------------------------------------
ARAth/1-205     ------------------------------------------------------------------------------------------------------------
CHLre/1-277     ------------------------------------------------------------------------------------------------------------
PLAfa/1-212   1 M-IRRSLIKLG-GYPKASFHEQHI-------NPFSNV-QWQSYPFLKKNMPK------------------V 43
TOXgo/1-231   1 M--WTSLLRLSQSYPKGSFHEGHI-------NPFADV-QWISRPFMKRNMPRD------------------H 44
THEpa/1-240   1 MFISKSLLA---RSLRSSFHEGNV-------NPFSKV-QWVSRPFLKKNLPT------------------V 42
TETth/1-391   1 MIGKNIVSKLGNLASNVHILNKQIASFSVWKNPTNYLPEKAKFPSPKELFPKDNENSWKTLNDLTPSLFKDV 72
PARte/1-357   1 MQLFQRCLVARFSLAIPKFKHKEQ--------PYVK---DIPMPKRPKLDPKDPYEKYELVK---PREYEFR 58
TRYbr/1-202   1 MQRSTRIVM--------------------APFKSV------LRRHKHHPEG------------------- 25
LEIma/1-171     ------------------------------------------------------------------------------------------------------------
```

Quality

```
HUMAN/1-178   1 ----------MSSFSRAPQQWAT-------------FARIWYLLDG----------------KMQPPGKLA 32
MOUSE/1-178   1 ----------MSSFSRAPQQWAT-------------FARMWYLLDG----------------KMQPPGKLA 32
DANre/1-179   1 ----------MSSFSRSAQQWAT-------------FARSWFLIDA----------------RMQPPGKIA 32
DROme/1-178   1 ----------MSIAKRVQQWAT-------------FARTWHIYDC----------------TWQNPFESA 31
ANIga/1-177   1 ----------L--FVAPFQQWAT-------------FARTWHIFDC----------------TWQNPFEAA 30
CAEel/1-205   2 -----SYRRAVSRFDRVNQWLQ-------------FSRQWHVIDA----------------NQQDAELLG 37
YEAST/1-163   1 ----------MSQKIGHSGLAF-------------ARLWHHVDVAR----------------DKRTLGRLA 32
NEUcr/1-183   1 ----------MSQTVGATRLAY-------------SRVWHHISAVTPHPTLSTIKAPSEAITPPSLGRLA 47
DICdi/1-227   1 ----------MSRAIFKNPLTS-------------SHLWHVIDA----------------SGHRVGRLA 30
ESCco/1-142   1 ----------MKTFTAKPETV-------------KRDWYVVDA----------------TGKTLGRLA 29
BRUsu/1-154   1 ----------MATFSQKPAEV-------------VKKWVLIDA----------------EGLVVGRLA 29
RICpr/1-155   1 ----------MKTYSAKPSEI-------------EKKWWVIDA----------------KNVVLGRLA 29
ARAth/1-205   1 ----------MATQAAAAASFKGNLKKAVAGIKRINLDGLRWRVFDA----------------RGQVLGRLA 46
CHLre/1-277   1 ----------MSRVTEAIKHLKDL--------QHIKLEGLRFRIIDA----------------KGQVVGRLA 38
PLAfa/1-212  44 DIFSEEHISKCALSVFDKE-------------KGNWFVIDA----------------TNKSVGSLA 80
TOXgo/1-231  45 HPLAKQHTSLKAVTMLDEES-------------GNHWHVLDG----------------KGRSVGGLA 82
THEpa/1-240  43 SPLATPHQSLGAITHMDTT-------------AGNWHIIDA----------------SNKTVGSIA 79
TETth/1-391  73 QGFKEKQVQRAAYMQIAKPN-------------GQMYHIFDA----------------SKMPLGRMC 110
PARte/1-357  59 QAL--DERHTKNFYPGTTYVAV-------------HKGGITYHLFDA----------------SRFPYGKMC 99
TRYbr/1-202  26 ----------LPLYNDMSKQW-------------LCREGERWWLLDA----------------RGEQLPRVA 58
LEIma/1-171   1 ----------MSKQW-------------LCREGERWWLLDA----------------RGQQLPHVA 27
```

Quality

```
HUMAN/1-178  33 AMASIRLQGLHKPVYHALS--DCGDHVVIMNTRHIAFSGNKWE---QKVY-SSHTGYPGGFRQVTAAQLHL- 97
MOUSE/1-178  33 VIASNKLQGLNKPVYHQLS--DCGDHVVIINTRHIAFSGNKWE---QKVY-SSHTGYPGGFRQVTAAQLHR- 97
DANre/1-179  33 SMCAVRLQGKHKPIYHPLS--DIGDHVVVMNTKHIAFSGNKWE---QKVY-SSHTGHPGSFKQVTAAQLHR- 97
DROme/1-178  32 KLVKTHLLGLQKPIYHPMN--DCGDHVVLINTREIALPGDEWV---KRVY-FHHTGYPGGASWTLAWQLHE- 96
ANIga/1-177  31 SLIRKHLMGLHKPIYHPMN--DCGDHVVVINTGEIALPGDEWK---KRAY-FHHTGYAGGATWTLAWQLHE- 95
CAEel/1-205  38 DKVARYLAGKHKPIFHPET--DCGDHVVTNCKDIAMHAFDWK---HTIY-KFNMEYPKSKADIPAWQIHD- 102
YEAST/1-163  33 SAIAITLIGRHKPVYHPSQ--DCGDYVVVTNCQKIRVTGKKFE---QKTY-WSHSGRPGQLKLQTMNKVVAD 98
NEUcr/1-183  48 SRIATILMGKHKPIWDPST--DCGDYVVVTNCAGLYTTGHKKW---RKTY-YRHNTRPGSLQAITMDALMEK 113
DICdi/1-227  31 TKISELLRGKHKPIYDRSVPLECGDYVVVLNAHKVEFTGKKWD---QKMY-RKHSGYPGGLKETLAKDMLV- 97
ESCco/1-142  30 TELARRLRGKHKAEYTPHV--DTGDYIIVLNADKVAVTGNKRT---DKVY-YHHTGHIGGIKQATFEEMIA- 94
BRUsu/1-154  30 SLVANRLRGKHKATFTPHV--DDGDNVIIINADKVVLTGKKYT---DKKY-YWHTGHPGGIKERTARQILEG 95
RICpr/1-155  30 SRVAIMLRGKHKPSFTPHL--DCGDNIIIINAEHIKLTGKKLNPKDGKVY-YRHTGFPGGIKDTTAGKILSG 98
ARAth/1-205  47 SQISTVLQAKDKPTYCPNR--DDGDICIVLNAKEIGFTGRKLT---DKFY-RWHTGYIGHLKERSLKDQMA- 111
CHLre/1-277  39 EQISVILQGKDKPTYNPTK--EQGDVVIVVNASHVELTHDKWN---TKLY-RWHTGYPGGLRSRPAGDQWE- 103
PLAfa/1-212  81 ACISKLLQGKYRVDYNPNK--VNSSSVVVNAIHVKFYGHTWD---TKIYKFPRKSHSKSHKILSCKTVFA- 146
TOXgo/1-231  83 AQVVRLLQGKHKRVDFTPRT--AAGDSVVVNAIHLKMAGHTWD---TKVYKFDRKTHPAGPKIITAKTIMA- 148
THEpa/1-240  80 SHVAVILQGKHLPTYQPNK--VTGDNVIIVNAIHVTMNGHSWD---TKVYKFDRKAHPKGPKIITAKTIMA- 145
TETth/1-391 111 QKIAFFLQGKHRPTFKNCD-QVTYDNIIVVNAANIMLTGKKAL---LKTV-KYHTGFVGGLKEKSYKFFLT- 176
PARte/1-357 100 SKIAYHLSGKHKPTFRNNEPGKVTDKFIIVNGCNMYLTGKKIN---YKVL-TYHTGYVGHLRQIKFRDLIL- 166
TRYbr/1-202  59 AVAAQYITGQHRPDFTPGM--ITGDHVVIVNIKDVVMVGDQWI---RVPI-TWQTAYPGGKYRIRLTDMYE- 123
LEIma/1-171  28 KIAAQYMTGQHRPDFTPGM--MTGDHVVITNIKDAVMTGDNWI---RVPI-TWQTAYPGGKYRVRLSEMYE- 92
```

Quality

S12

Figure S1A continuation

Figure S1A continuation

```
HUMAN/1-178    174 - - - - - - - - - E D Y R L - - - - - - - - - - - - - - - - - - - - - - - - - - - - - - - - - - - - - - - - 178
MOUSE/1-178    174 - - - - - - - - - D D F R M - - - - - - - - - - - - - - - - - - - - - - - - - - - - - - - - - - - - - - - - 178
DANre/1-179    174 - - - - - - - - - E D Y R M K - - - - - - - - - - - - - - - - - - - - - - - - - - - - - - - - - - - - - - 179
DROme/1-178    173 - - - - - - - - - K D Y I L R - - - - - - - - - - - - - - - - - - - - - - - - - - - - - - - - - - - - - - 178
ANIga/1-177    172 - - - - - - - - - K D Y I L R - - - - - - - - - - - - - - - - - - - - - - - - - - - - - - - - - - - - - - 177
CAEel/1-205    179 - - - - - - - - - D K H V V D W E K S - - - - - - - - - - - - - - - - - - - - - - - - - - I P N P G R - - - - - 194
YEAST/1-163        - - - - - - - - - - - - - - - - - - - - - - - - - - - - - - - - - - - - - - - - - - - - - - - - - - - - - - -
NEUcr/1-183        - - - - - - - - - - - - - - - - - - - - - - - - - - - - - - - - - - - - - - - - - - - - - - - - - - - - - - -
DICdi/1-227    192 R S H K D Q L K R E R R L L R K K R V N E L - - - - - - - - - - - - - - - - - - - - - - - - - - - - - - - - 213
ESCco/1-142        - - - - - - - - - - - - - - - - - - - - - - - - - - - - - - - - - - - - - - - - - - - - - - - - - - - - - - -
BRUsu/1-154        - - - - - - - - - - - - - - - - - - - - - - - - - - - - - - - - - - - - - - - - - - - - - - - - - - - - - - -
RICpr/1-155        - - - - - - - - - - - - - - - - - - - - - - - - - - - - - - - - - - - - - - - - - - - - - - - - - - - - - - -
ARAth/1-205    194 - - - - - - - - K G K K R T L S E V P A - - - - - - - - - - - - - - - - - - - - - - - - - - - - - - - - - - 205
CHLre/1-277    232 G A S G S G S G R Q Q R Q R P T V P I D D L L - - - - - - - - - - - - - - - T E E E - - - - - - - - - - - - 258
PLAfa/1-212        - - - - - - - - - - - - - - - - - - - - - - - - - - - - - - - - - - - - - - - - - - - - - - - - - - - - - - -
TOXgo/1-231    224 - - - - - - - L G D R M K M E - - - - - - - - - - - - - - - - - - - - - - - - - - - - - - - - - - - - - - - 231
THEpa/1-240    222 G A A G P S L S T D Q L C Y T L Y P V - - - - - - - - - - - - - - - - - - - - - - - - - - - - - - - - - - 240
TETth/1-391    381 A A K G G K Q G G K K - - - - - - - - - - - - - - - - - - - - - - - - - - - - - - - - - - - - - - - - - - 391
PARte/1-357    254 - - - - - - - - D I K Q Q I M D P S E L D N D L I F T P F V E R P Q K I K L N M T Q H E Y D K L N R R R K R L M Q R Y R K Y M P I P Y R N T I E K 318
TRYbr/1-202        - - - - - - - - - - - - - - - - - - - - - - - - - - - - - - - - - - - - - - - - - - - - - - - - - - - - - - -
LEIma/1-171        - - - - - - - - - - - - - - - - - - - - - - - - - - - - - - - - - - - - - - - - - - - - - - - - - - - - - - -

Quality
```

```
HUMAN/1-178        - - - - - - - - - - - - - - - - - - - - - - - - - - - - - - - - - - - - - - - - - -
MOUSE/1-178        - - - - - - - - - - - - - - - - - - - - - - - - - - - - - - - - - - - - - - - - - -
DANre/1-179        - - - - - - - - - - - - - - - - - - - - - - - - - - - - - - - - - - - - - - - - - -
DROme/1-178        - - - - - - - - - - - - - - - - - - - - - - - - - - - - - - - - - - - - - - - - - -
ANIga/1-177        - - - - - - - - - - - - - - - - - - - - - - - - - - - - - - - - - - - - - - - - - -
CAEel/1-205    195 - - - - - - - - - - - - - H V K P V P G Q K D K - - - - - - - - - - - - - - -                205
YEAST/1-163        - - - - - - - - - - - - - - - - - - - - - - - - - - - - - - - - - - - - - - - - - -
NEUcr/1-183        - - - - - - - - - - - - - - - - - - - - - - - - - - - - - - - - - - - - - - - - - -
DICdi/1-227    214 - - - - - - - - - - - - - - - - - - - - - K P L R S P P K T E E I D N - -                227
ESCco/1-142        - - - - - - - - - - - - - - - - - - - - - - - - - - - - - - - - - - - - - - - - - -
BRUsu/1-154        - - - - - - - - - - - - - - - - - - - - - - - - - - - - - - - - - - - - - - - - - -
RICpr/1-155        - - - - - - - - - - - - - - - - - - - - - - - - - - - - - - - - - - - - - - - - - -
ARAth/1-205        - - - - - - - - - - - - - - - - - - - - - - - - - - - - - - - - - - - - - - - - - -
CHLre/1-277    259 - - - - - - - - - - R A A L A A V E G G K G K S G A S S S - - - - - - - - -                277
PLAfa/1-212        - - - - - - - - - - - - - - - - - - - - - - - - - - - - - - - - - - - - - - - - - -
TOXgo/1-231        - - - - - - - - - - - - - - - - - - - - - - - - - - - - - - - - - - - - - - - - - -
THEpa/1-240        - - - - - - - - - - - - - - - - - - - - - - - - - - - - - - - - - - - - - - - - - -
TETth/1-391        - - - - - - - - - - - - - - - - - - - - - - - - - - - - - - - - - - - - - - - - - -
PARte/1-357    319 A D F T K S Y V V K S E K Q L N R L G L Q K I K P L D D D P E L E D E T T K F                357
TRYbr/1-202        - - - - - - - - - - - - - - - - - - - - - - - - - - - - - - - - - - - - - - - - - -
LEIma/1-171        - - - - - - - - - - - - - - - - - - - - - - - - - - - - - - - - - - - - - - - - - -

Quality
```
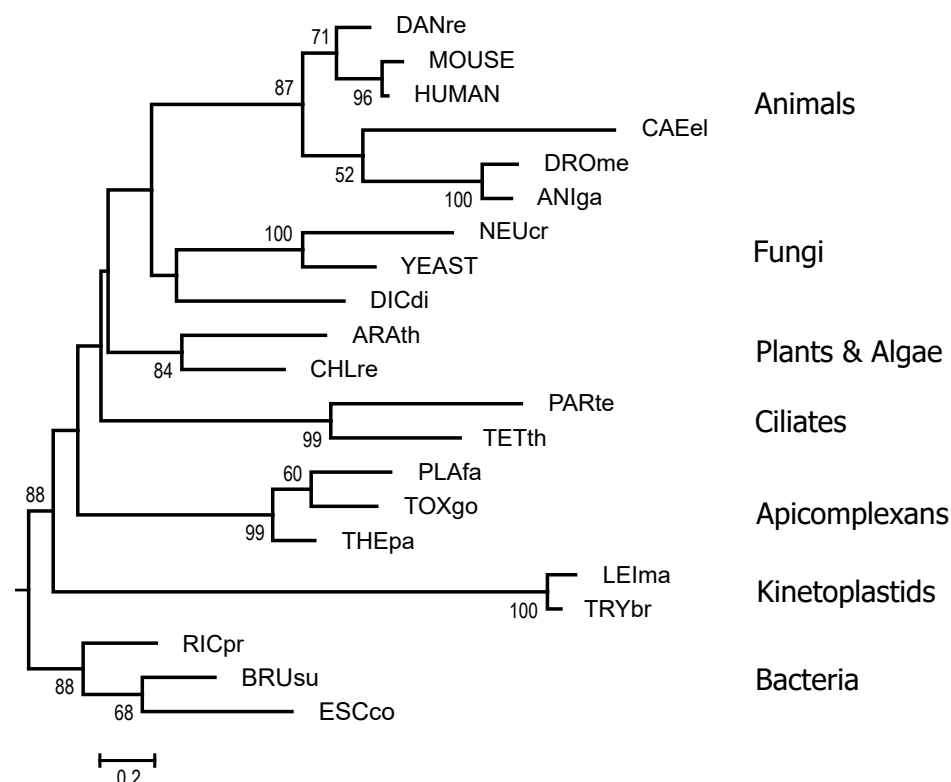
Figure S1B

Figure S1. (A) Multiple sequence alignment of a representative set of mitochondrial RPL13 proteins from a broad range of phyla and sample proteobacterial RPL13 proteins ("outgroup"). The proteins chosen mirror those used in a previous study of mitoribosomal proteins (11), with the addition of three alveolate proteins (*Toxoplasma gondii*, *Theileria parva*, *Paramecium tetraurelia*) and one vertebrate (*Danio rerio*) and removal of the vertebrate *Tetraodon nigroviridis*. Sequence alignment was performed with the MAFFT server using L-INS-i method and homologues addition (12). The alignment was formatted for display with JALVIEW using the Clustal color scheme, which reflects the chemical property of conserved amino acids at each alignment position (13). The solid red bars indicate the columns of the alignment that match the Interpro family model "Ribosomal Protein L13, bacterial-type" (IPR005823) (which model includes mitochondrial and chloroplast L13 subunits). Specific IDs of the protein sequences aligned (UniProt designations): HUMAN (*Homo sapiens*)Q9BYD1, MOUSE (*Mus musculus*) Q9D1P0, *Danio rerio*Q504D1, *Drosophila melanogaster*Q9VJ38, *Anopheles gambiae* Q7Q191, *Caenorhabditis elegans*Q95QL2, YEAST (*Saccharomyces cerevisiae*) Q12487, *Neurospora crassa*Q7SBV6, *Dictyostelium discoideum*Q554U7, *Arabidopsis thaliana*Q7XA68, *Chlamydomonas reinhardtii*A8J810, *P. falciparum*O96222, *T. gondii* A0A125YJY5, *T. parva*Q4N8U5, *Tetrahymena thermophila*W7X626, *P. tetraurelia*A0C5X1, *Trypanosoma brucei* Q580D5, *Leishmania major* Q4Q2H6, *Escherichia coli* P0AA10, *Brucella suis*Q8G1C8, and *Rickettsia prowazekii*Q9ZDU1.

(B) Phylogenetic tree inferred for the set of diverse mitochondrial RPL13 and proteobacterial RPL13 sequences. Apicomplexan mRPL13 subunits form a well-supported, separate clade within the mitochondrial grouping (the latter defined by setting the root with the proteobacterial clade). The tree was inferred by maximum likelihood analysis (PhyML(14)). Bootstrap support is shown for nodes with greater than 50% support.
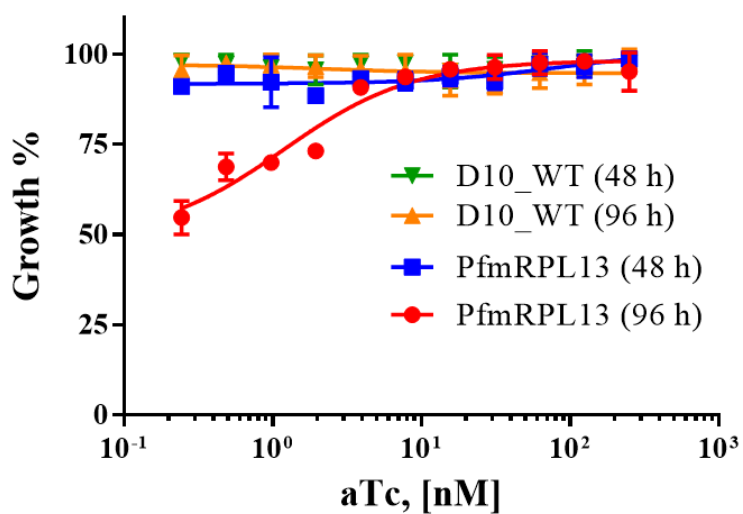
Figure S2. Growth of PfmRPL13 knockdown parasites with various concentrations of aTc for one and two cycles using ^{3}H-hypoxanthine incorporation. aTc was diluted from 250 nM in a serial dilution with a factor of 2. The lowest concentration was 0.24 nM. D10 wildtype served as a control. Error bars were derived from n=3 biological replicates.
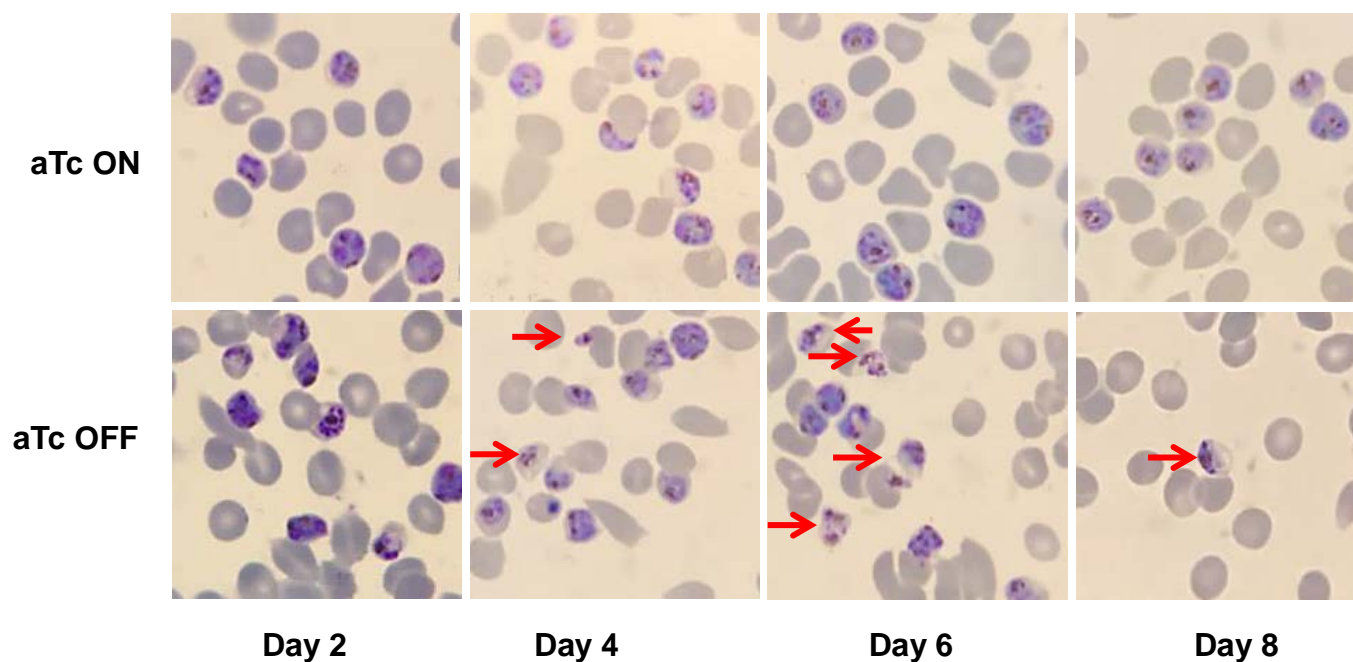
Figure S3. Morphological changes of PfmRPL13 knockdown parasites on Giemsa stained thin blood smears. Red arrows indicate dead or morphologically deteriorating parasites after aTc was removed from the culture. To display multiple parasites in one field under the microscope, late stage parasites of the cultures with or without aTc were enriched by a Percoll gradient.
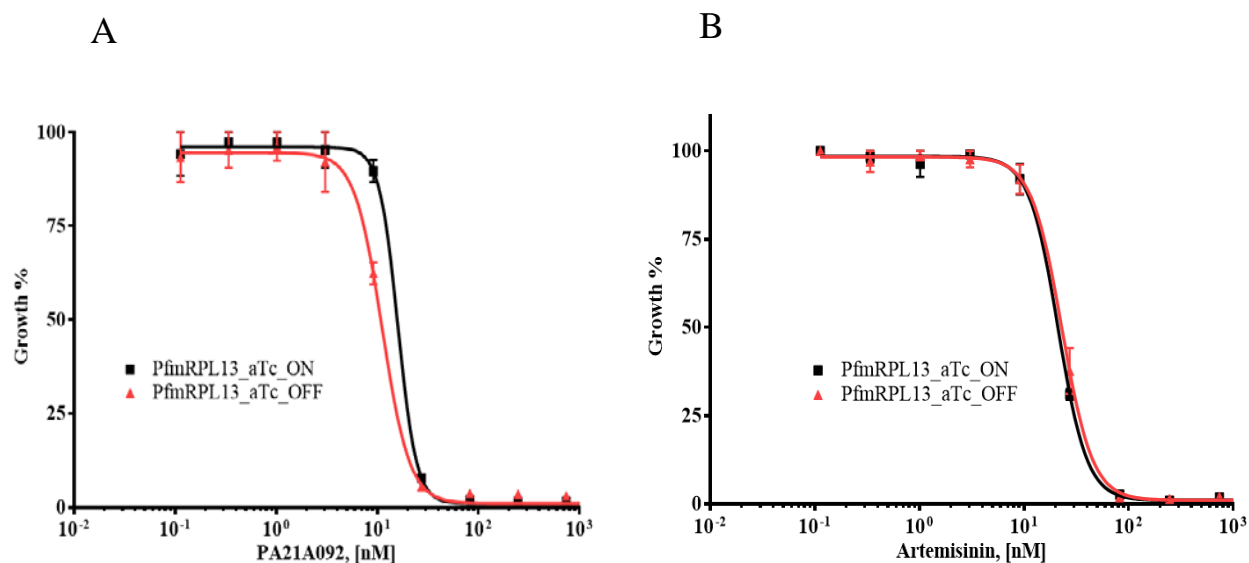
Figure S4. PfmRPL13 knockdown parasites show equal sensitivity to PA21A092 and artemisinin in the presence or absence of aTc. Growth inhibition assays were carried out using ^{3}H-hypoxanthine incorporation in 48 h. PfmRPL13 knockdown parasites were grown in the absence of aTc for 3 cycles before exposed to PA21A092 (15) or artemisinin. EC50s of PA21A092 in the presence or absence of aTc are 15.9 nM and 11.2 nM, respectively. EC50s of artemisinin in the presence or absence of aTc are 21.2 nM and 23.1 nM, respectively.

aTc ON
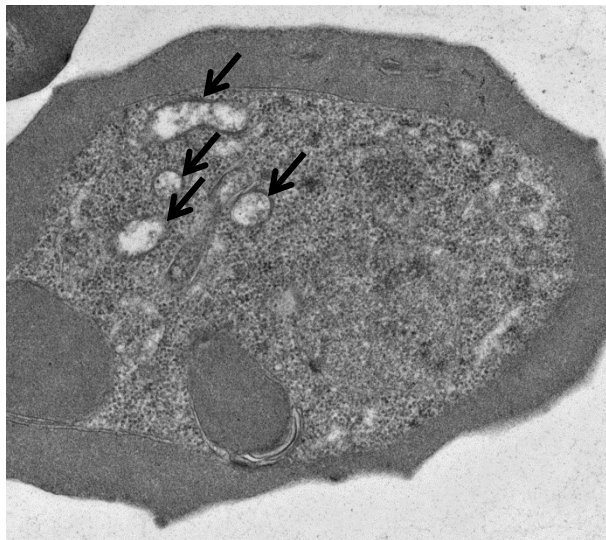
aTc OFF
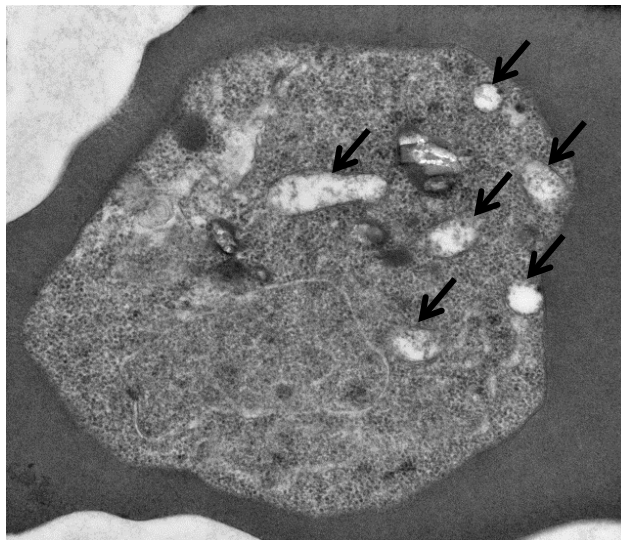
D10 wildtype

Figure S5. Mitochondrial morphologies of D10 wildtype parasites maintained with or without aTc and examined by transmission electron microscopy (TEM) studies. Black arrows on TEM images indicate cross sections of the parasite mitochondria.

References

1. Balabaskaran Nina P, Morrisey JM, Ganesan SM, Ke H, Pershing AM, Mather MW, Vaidya AB. 2011. ATP synthase complex of Plasmodium falciparum: dimeric assembly in mitochondrial membranes and resistance to genetic disruption. J Biol Chem 286:41312-22.
2. Nkrumah LJ, Muhle RA, Moura PA, Ghosh P, Hatfull GF, Jacobs WR, Jr., Fidock DA. 2006. Efficient site-specific integration in Plasmodium falciparum chromosomes mediated by mycobacteriophage Bxb1 integrase. Nat Methods 3:615-21.
3. Ghorbal M, Gorman M, Macpherson CR, Martins RM, Scherf A, Lopez-Rubio JJ. 2014. Genome editing in the human malaria parasite Plasmodium falciparum using the CRISPR-Cas9 system. Nat Biotechnol 32:819-21.
4. Ganesan SM, Falla A, Goldfless SJ, Nasamu AS, Niles JC. 2016. Synthetic RNA-protein modules integrated with native translation mechanisms to control gene expression in malaria parasites. Nat Commun 7:10727.
5. Spillman NJ, Beck JR, Ganesan SM, Niles JC, Goldberg DE. 2017. The chaperonin TRiC forms an oligomeric complex in the malaria parasite cytosol. Cell Microbiol 19.
6. Painter HJ, Morrisey JM, Mather MW, Vaidya AB. 2007. Specific role of mitochondrial electron transport in blood-stage Plasmodium falciparum. Nature 446:88-91.
7. Adjalley SH, Johnston GL, Li T, Eastman RT, Ekland EH, Eappen AG, Richman A, Sim BK, Lee MC, Hoffman SL, Fidock DA. 2011. Quantitative assessment of Plasmodium falciparum sexual development reveals potent transmission-blocking activity by methylene blue. Proc Natl Acad Sci U S A 108:E1214-23.
8. Ke H, Lewis IA, Morrisey JM, McLean KJ, Ganesan SM, Painter HJ, Mather MW, Jacobs-Lorena M, Llinas M, Vaidya AB. 2015. Genetic investigation of tricarboxylic acid metabolism during the Plasmodium falciparum life cycle. Cell Rep 11:164-74.
9. Mather MW, Morrisey JM, Vaidya AB. 2010. Hemozoin-free Plasmodium falciparum mitochondria for physiological and drug susceptibility studies. Mol Biochem Parasitol 174:150-3.
10. Ke H, Morrisey JM, Ganesan SM, Painter HJ, Mather MW, Vaidya AB. 2011. Variation among Plasmodium falciparum strains in their reliance on mitochondrial electron transport chain function. Eukaryot Cell 10:1053-61.
11. Smits P, Smeitink JA, van den Heuvel LP, Huynen MA, Ettema TJ. 2007. Reconstructing the evolution of the mitochondrial ribosomal proteome. Nucleic Acids Res 35:4686-703.
12. Katoh K, Rozewicki J, Yamada KD. 2017. MAFFT online service: multiple sequence alignment, interactive sequence choice and visualization. Brief Bioinform doi:10.1093/bib/bbx108.
13. Waterhouse AM, Procter JB, Martin DM, Clamp M, Barton GJ. 2009. Jalview Version 2--a multiple sequence alignment editor and analysis workbench. Bioinformatics 25:1189-91.
14. Guindon S, Dufayard JF, Lefort V, Anisimova M, Hordijk W, Gascuel O. 2010. New algorithms and methods to estimate maximum-likelihood phylogenies: assessing the performance of PhyML 3.0. Syst Biol 59:307-21.
15. Das S, Bhatanagar S, Morrisey JM, Daly TM, Burns JM, Jr., Coppens I, Vaidya AB. 2016. Na+ Influx Induced by New Antimalarials Causes Rapid Alterations in the Cholesterol Content and Morphology of Plasmodium falciparum. PLoS Pathog 12:e1005647.